AN ABSTRACT OF THE THESIS OF

Allison Ruth Northcutt for the degree of Master of Science in General Science presented on 2 June 1986.

Title: In Vivo Counting of Americium-241 in Human Lungs and Tracheobronchial Lymph Nodes[1]

Redacted for Privacy

Abstract approved: Stephen E. Binney

To distinguish americium-241 in human lungs from translocated activity in the tracheobronchial lymph nodes (TBLN), two intrinsic germanium detectors were collimated with 0.3-cm lead sheeting. A tissue-equivalent phantom containing either 620 nCi (22.9 kBq) in the lungs or a 2200 nCi (81.4 kBq) TBLN point source was counted; as chest wall thickness increased, net count rate per unit activity generally decreased exponentially for two of three counting positions. Phantom calibration curves were compared to data obtained by the same detection system for a human male with a known lung deposition of 2.4 nCi (88.8 Bq) of americium-241. The relation of the data to the calibration curves indicated the activity was restricted

to the lungs. If activity had translocated to the smaller TBLN, the specific dose would have increased and the TBLN might have been designated the critical organ.

[1]This research was supported by the Northwest College and University Association for Science (University of Washington) under Contract DE-AMØ6-76-RLO2225 with the U. S. Department of Energy.

In Vivo Counting of Americium-241 in Human Lungs and Tracheobronchial Lymph Nodes

by

Allison Ruth Northcutt

A THESIS

submitted to

Oregon State University

in partial fulfillment of
the requirements for the
degree of

Master of Science

Completed 2 June 1986

Commencement June 1987

APPROVED:

Redacted for Privacy

Associate Professor of Nuclear Engineering in charge of major

Redacted for Privacy

Chairman of Department of General Science

Redacted for Privacy

Dean of Graduate School

Date thesis is presented 2 June 1986

Acknowledgements

My time in Oregon has been enhanced by the friendships and associations of numerous people. Each person has uniquely contributed to my graduate school experience and has made the Oregon sojourn a cherished event. To Dr. David Willis, I thank him for granting me a teaching assistantship that allowed me to "go west." To the TA's, I thank them for their humor and patience: Carrie, Andy, Gail, Mary, P. J., Lisa, James, Dave, Bill, Terria, Susan, Dennis, and Larry. To Keith King, Nan Field, Jack Lyford, and Henry VanDyke, I thank them for sharing their teaching skills and enthusiasm for the GS courses. To Orysia Dawydiak and David Sims, I thank them for their friendship and giving me some "farm experience."

The summer I spent in Richland enabled me to conduct my thesis research and work with Earl Palmer. I thank him for his encouragement and willingness to share his time and skills with me. Moreover, his staff at Battelle was extremely helpful and considerate of my thesis work.

Of course, this research project would not have been possible without the supervision of Dr. Stephen Binney. As my major professor, he kindly guided me along whenever I went astray and provided needed assistance with all phases of this thesis. I appreciate

the time and dedication he devoted to me and my learning experience.

Across the miles, my parents, brothers (Henry and Douglas), and Jimmy and other special friends have given me support in my graduate school endeavor. The frequent letters and phone calls bridged the 3000 miles and kept me in touch with home and family.

TABLE OF CONTENTS

LIST OF FIGURES

LIST OF TABLES

In Vivo Counting of Americium-241 in Human Lungs and Tracheobronchial Lymph Nodes

Chapter 1. Introduction

During the last years of World War II, scientists working for the government of the United States developed and tested atomic explosives and bombs. Later, Dr. J. Robert Oppenheimer, one of the senior scientists, commented on the advent of the nuclear age. "In the hour before dawn one day in the summer of 1945, the hills of Jornado del Muerta, a desert stretch in New Mexico, were briefly lighted with a light no man had ever seen before. We who were there knew that a new world lay before us" (Oppenheimer 1947).

This new world has evolved to include peacetime uses of nuclear energy and radiation such as in electrical power production, medical diagnosis and therapeutics, scientific research, and industrial goods and services, as well as the continued production of nuclear weapons. With respect to nuclear weapons, personnel working with plutonium production, separation, and recovery are monitored for potentially inhaled or ingested radioactive particles. This monitoring program assists in maintaining a safe working environment for the personnel handling plutonium and its by-products. One of these by-products is americium.

The Whole Body Counting Unit of Battelle Pacific Northwest Laboratories in Richland, Washington, operates a unique detection and counting system to measure radioactivity in the lungs. As part of the safety monitoring program, certain nuclear personnel are routinely measured for radioactivity in the lungs. If an inhalation incident should occur, this unit has the capability to detect and measure inhaled radioactive particles.

Animal studies have shown that insoluble radioactive particles may migrate or translocate from the lung to lymph nodes surrounding the trachea. To attempt to measure radiation emitted only from this restricted region of the lymph nodes, the following criteria were established for this study:

1) Design a shield (or collimator) to permit only radiation from the lymph node region to enter the detectors in order to attempt to distinguish activity in the lungs from activity in the lymph nodes.

2) Calibrate the collimated detection system with a tissue-equivalent phantom containing known amounts of americium-241 activity in the lung and the lymph nodes.

3) Compare the phantom calibration data to a human male subject with a known americium-241 deposition.

4) Evaluate the male subject counting results and determine to what degree translocation of insoluble radioactive particles might have occurred.

Americium-241

Americium, atomic number 95, is the third element past uranium in the periodic table and has documented isotopes varying in atomic mass from 232 to 247.

Americium was discovered in late 1944 by Seaborg, Ghiorso, James, and Morgan while working at the wartime metallurgical laboratory at the University of Chicago (Schulz 1976). Less than a year after the initial discovery, Cunningham isolated americium in pure form as a compound, $Am(OH)_3$, and measured its absorption spectrum in an aqueous solution.

Americium-241 is produced by the following nuclear reactions:

$$^{239}Pu\ (n, \gamma)\ ^{240}Pu\ (n, \gamma)\ ^{241}Pu \xrightarrow{\beta^-} {}^{241}Am$$

Americium-241 decays by both alpha particles and gamma rays with a half-life of 432.2 years. The 59.6 keV gamma ray (abundance 36%) and the neptunium L x-ray (about 18 keV following internal conversion) predominate the photon spectrum.

Americium is recovered and purified as a result of normal reworking of aged plutonium inventories containing various amounts of the plutonium-241 isotope (Schulz 1976). Sites of recovery in the United States incude the Department of Energy facilities at Rocky Flats (Colorado), Hanford (Washington), and Los Alamos (New Mexico).

Anatomy of the Respiratory Tract

The human lungs, weighing about 1 kg, are pinkish-gray in color with darker areas depending on the amount of inhaled and retained particulates (Jacquez 1978). The right lung is divided into three lobes: superior, middle, and inferior. The left lung has two lobes: superior and inferior (Figure 1). The visceral pleural membrane covers the lungs, and the parietal pleural membrane lines the chest wall (Weibel 198Ø). The visceral pleura rests closely on the parietal pleura with only a thin film of serous fluid (a lubricant) between the two surfaces.

The respiratory system is divided into three main levels: nasopharyngeal, tracheobronchial, and pulmonary (TGLD 1966). Air enters the respiratory tract through the anterior nares that have course hairs to trap or impede larger particles (Stuart 1984). As the aerosol passes through the posterior nares, the particles are warmed and humified over the flattened projections or the chonchae. Particles enter the nasopharyngeal region which extends from the oral pharynx to the larynx (Figure 2). The trachea descends from the larynx and is lined with ciliated epithelium containing mucus-producing goblet cells. Sixteen to twenty C-shaped cartilages in the wall support the trachea. The trachea divides into right and left bronchi that also contain

Figure 1. Membranes and lobes of the human lung.

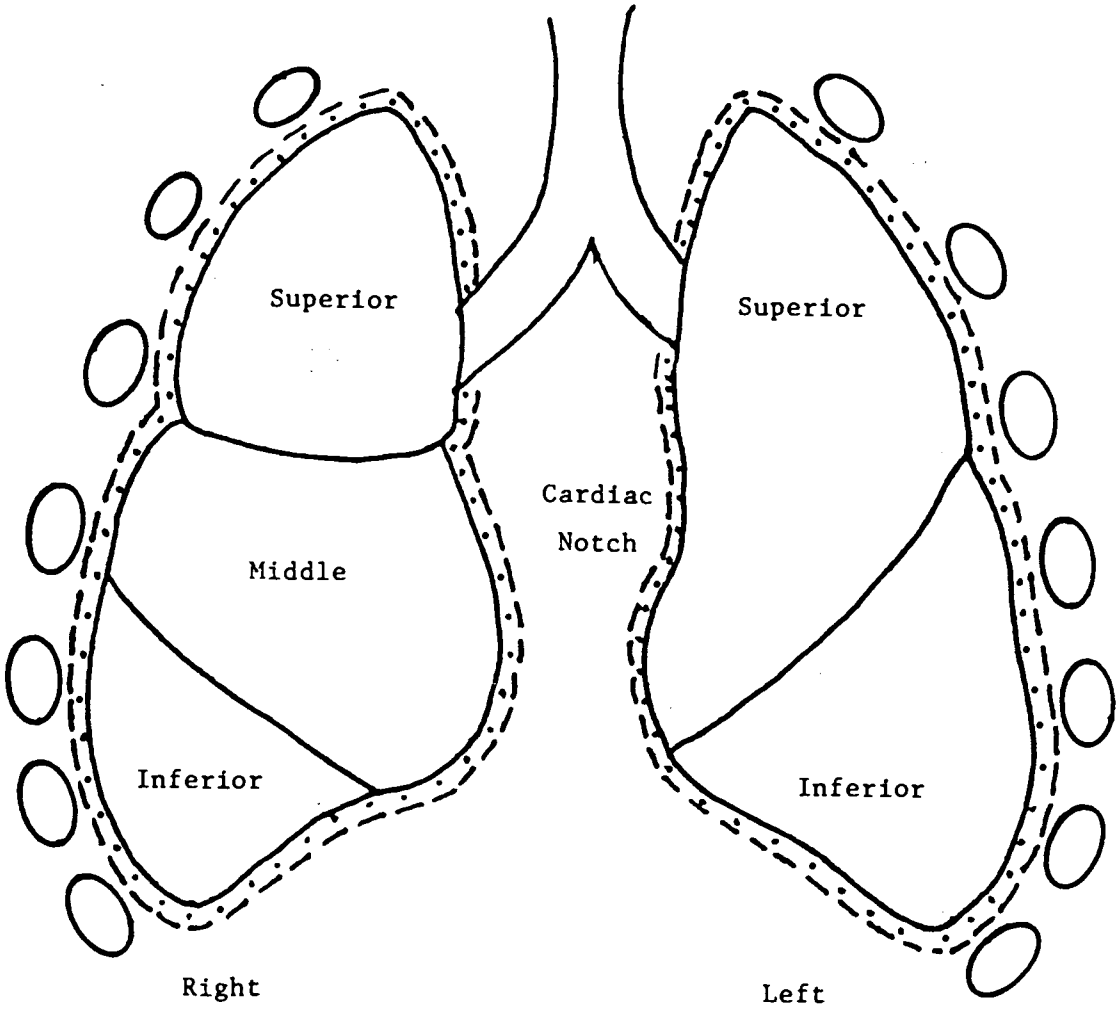

. . . Visceral Pleural Membrane

----- Parietal Pleural Membrane

(Adapted from: D. Shepro, F. Belamarich, and C. Levy, Human Anatomy and Physiology. A Cellular Approach).

Figure 2. The human respiratory tract.

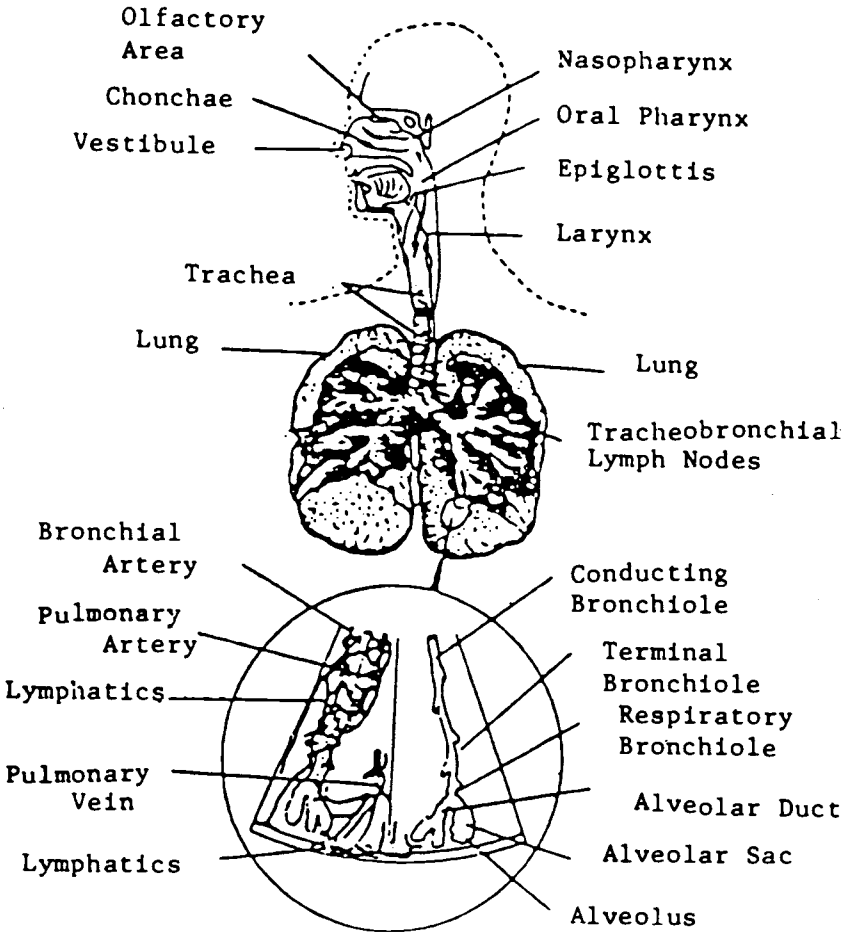

(Adapted from: B. O. Stuart, "Deposition and clearance of inhaled particles," Env. Health Persp. 55, 369-390).

cartilaginous plates in an irregular pattern (Jacquez 1979). These bronchi separate into secondary lobar branches and subsegmented branches numbering about 800 (Stuart 1984). Branching continues to form smaller conducting airways that contain goblet cells and secretory glands but no cartilaginous plates. These branches or bronchioles occur after about 11 generations of branching (Jacquez 1979). Eventually the goblet cells and glands disappear and the lining becomes non-ciliated at the terminal bronchioles. The terminal bronchioles, the last division of a purely conductive airway, separate into non-ciliated respiratory bronchioles and number about 15,000 (Jacquez 1979). Respiratory bronchioles, sites of gas exchange, further divide into alveolar ducts; 26 million ducts give rise to a total of 50 to 100 million alveolar sacs that are composed of 300 million alveoli (Weibel 1980). These sacs provide 30 to 100 m^2 of gas exchange surface in human adults, depending on body size and exercise level (Stuart 1984). Retention and elastic fibers compose the alveolar walls which support fine pulmonary capillaries.

Lymphatics

The alveoli are packed closely together with only thin, alveolar septa between them (Weibel 1980). Blood in a single network of capillaries occupies the septa; therefore, blood is exposed to air on two sides through

three layers: an alveolar epithelium, a capillary endothelium, and an intercalated interstitial layer that contains supporting fibers.

Lymphatic ducts begin in the region of the alveolar ducts and respiratory bronchioles and are not found with the alveoli and alveolar sacs (Fraser and Pare 1971). The deep or parenchymatous lymphatic drainage system begins as blind capillaries at the alveolar duct. Some of these lymphatic capillaries also abut on bronchioles, pulmonary blood vessels, visceral pleura, and interlobar septa (Morrow 1980). Thus interstitial fluid seeping from blood capillaries drains along connective tissue and into lymph capillaries (Weibel 1980). Lymph vessels continue through the lung with lymph nodes serving as filters. Lymph moves toward the tracheal bifurcation (location of the tracheobronchial lymph nodes), (Figure 3), and along the trachea into the right and left mediastinal channels; the right channel drains into the subclavian vein and the left, together with the thoracic duct, drains into the left subclavian vein (Weible 1980).

The superficial or visceral pleural lymphatic drainage system drains similarly to the deep system but has a smaller capacity and is near the lung surface (Morrow 1980). Thus lymph in the lung eventually empties directly into the blood system.

Figure 3. Tracheobronchial lymph nodes (TBLN) of the human respiratory tract.

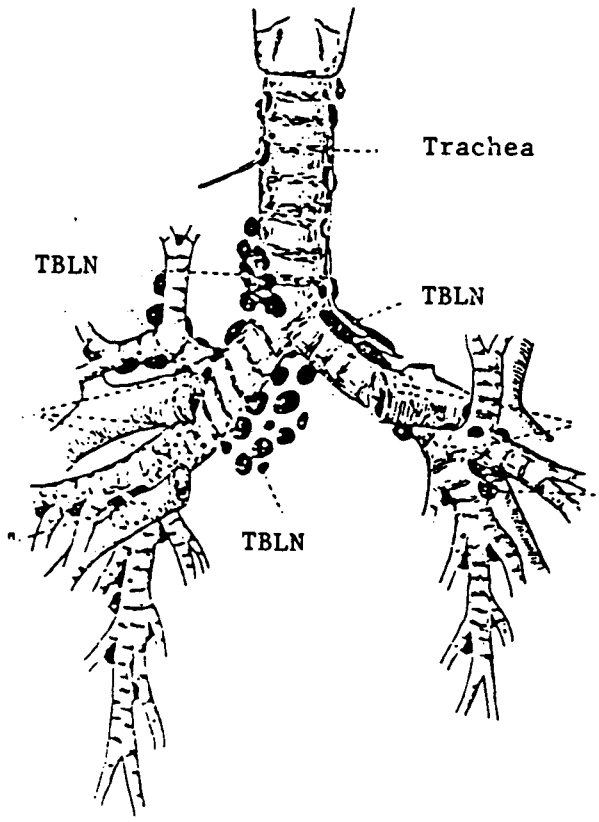

(Adapted from: C. Naguishi, Functional Anatomy and Histology of the Lung).

Lymph is a transparent, straw-colored fluid composed of interstitial fluid (95% water), proteins (such as albumin, globulin, and fribrinogen), and lymphocytes (Eckert and Randall 1983). Lymph is collected from almost all body tissues and returns excess fluid and protein to the blood. Moreover, the lymph nodes produce lymphocytes and monocytes that defend the body from infection. Smooth muscle surrounding the larger lymphatic vessels, contractions of the gut and the skeletal muscles, and general body movement cause the lymph to flow. Although the lymph fluid flow rate varies, the average rate is 11 ml/hr for resting individuals. This value is 1/3000 of the average cardiac output.

Particulate Deposition and Clearance

Deposition is defined as the amount of material in inspired air that remains after expiration. Inhalation consists of three principal mechanisms of deposition: inertial impaction, sedimentation, and diffusion (Stuart 1984). Rates of air flow, residence time in the various levels of the respiratory tract, particle size, and concentration influence the modes of deposition (Stuart 1984, Bair and Willard 1963). Inertial impaction involves large particle sizes in the upper respiratory tract with diameters ranging in size from 2 microns to >20 microns (Stuart 1984). The inertia of the particle

tends to maintain the initial path if the air stream is deflected by nasal turbinates or branching airways. Sedimentation involves particles settling under the force of gravity and generally affects particles with diameters ranging from 0.1 micron to 50 microns (Stuart 1984). These particles mainly deposit in the small bronchi and bronchioles. Very small particles ranging from 0.5 micron to <0.002 micron deposit in the gas exchange areas of the lung by diffusion or Brownian motion (Stuart 1984). Random thermal motion of the gas molecules displaces the particles.

Lung clearance of inhaled dust and particles is a continuous process involving the three regions of the respiratory tract: nasopharynx, tracheobronchial, and pulmonary (Stuart 1984,TGLD 1966). Three primary clearance paths route the particles to the blood, the lymphatics, and the gastrointestinal (GI) tract: a) direct particle dissolution from the lungs into the bloodstream, b) macrophage movement of particles to the lymph capillaries, and c) mucociliary transport of particles that are eventually swallowed.

Insoluble particles deposited on the surface of the nasopharynx or trachea regions may be cleared by mucociliary transport or pulmonary alveolar macrophages and moved to the nasopharynx and swallowed. This material then passes through the GI tract (Stuart 1984).

Insoluble particles below the ciliated airways or in the alveolar region are commonly cleared by alveolar macrophages (Murray 1976). The macrophages phagocytize (digest) the material or carry the particle along the mucociliary transport system and are eventually swallowed. The alveolar macrophage may follow a second route and move through the interstitial space of the inter-alveolar septa until the macrophage reenters near the respiratory and terminal bronchioles. Some macrophages enter the lymphatic capillaries instead of the bronchioles (Murray 1976). The mechanism for macrophage transfer from the alveolar surface to the interstitial space is unknown (Weibel 1980).

Soluble particles may be absorbed directly into the bloodstream after dissolution within the airway lining fluids or cells (Stuart 1984). This process may occur in all regions of the vascularized respiratory tract. Excretion clearance routes include fecal and urinary pathways that remove particles located in the blood or absorbed into the blood through the GI tract.

Lung Dynamics Models

In 1959, the International Commission on Radiological Protection (ICRP) developed a working lung dynamic model to describe the deposition of inhaled dust (TGLD 1966). Included was the assumption that 75% of the mass of the inhaled soluble and insoluble dust was

deposited in the respiratory tract and 25% of the mass was exhaled. For the 75% soluble dust deposited, 2/3 was assumed to rapidly pass into the GI tract and 1/3 entered the blood circulation. For the 75% insoluble dust deposited, 2/3 was also assumed to pass into the GI tract, with 1/6 of the remaining dust passing rapidly into the GI tract during the first day and 1/6 being retained in the respiratory tract for relatively long retention times. A general effective biological half-life of 120 days was assigned to all radionuclides except plutonium (1 year) and thorium (4 years). This model failed to describe kinetically all rapid clearance mechanisms or the kinetics of lymph dust clearance.

Later, the ICRP recognized the simplistic approach of this model and the need for more detailed criteria. In 1966, the ICRP created the Task Group on Lung Dynamics (TGLD) to develop a deposition model for inhaled particles. The task group identified the purpose of the model as "computing dust deposition in and clearance from the human respiratory tract, thereby providing a basis for lung dosimetry and the setting of exposure limits" (TGLD 1966). Three compartments, or sites of deposition, were chosen to represent the respiratory tract: nasopharynx (N-P), or the anterior and posterior nares to the larynx; tracheobronchial (T-B), or the trachea and bronchial tree to and includ-

ing the terminal bronchioles; and the pulmonary (P) region with the alveolar ducts, sacs, and alveoli. A fourth region, the lymphatics (L), was also identified as a respiratory region. The TGLD concluded that dust deposited directly on the ciliated surfaces would have clearance half-times of the order of minutes. A rapid clearance phase (about a 24-hour half-time) would apply to the alveolar region due to phagocytosis and muco-ciliary transport. A slower alveolar clearance phase would depend on the physicochemical properties of the dust as well as other properties such as particle size. The lymph clearance mechanism was fractionated, with some material retained in the lymph nodes and other material entering the blood. Thus a model was developed to include dust deposition sites, clearance pathways, biological half-times, and compartmental fractions for an aerosol with an AMAD of 1 micron (Figure 4). AMAD (activity median aerodynamic diameter), " is the diameter of a unit density sphere with the same terminal settling velocity in air as that of the aerosol particle whose activity is the median for the entire aerosol" (ICRP 3Ø).

The task group also evaluated several chemical elements and placed them into one of three possible categories that generally predicted time for clearance from the pulmonary region:

Figure 4. Task Group on Lung Dynamics model to describe clearance pathways from the respiratory system.

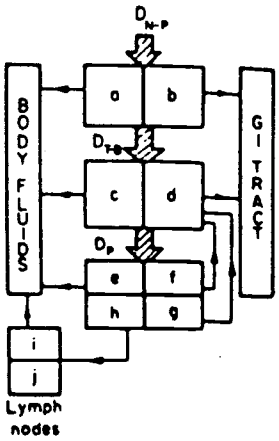

		D	D	Class W	W	Y	Y
Region	Compartment	T	F	T	F	T	F
N–P	a	0.01	0.5	0.01	0.1	0.01	0.01
(Dn–p = 0.30)	b	0.01	0.5	0.40	0.9	0.40	0.99
T–B	c	0.01	0.95	0.01	0.5	0.01	0.01
(Dt–b = 0.08)	d	0.2	0.05	0.2	0.5	0.2	0.99
	e	0.5	0.8	50	0.15	500	0.05
P	f	na	na	1.0	0.4	1.0	0.4
(Dp = 0.25)	g	na	na	50	0.4	500	0.4
	h	0.5	0.2	50	0.05	500	0.15
L	i	0.5	1.0	50	1.0	1000	0.9
	j	na	na	na	na	∞	0.1

Note: Removal depositions of an aerosol with an AMAD of 1 micron (Dn–p, Dt–b, and Dp), the removal half–times (Ta–j), and the compartmental fractions (Fa–j) are given in the tabular portion of the table. Classes D, W, and Y refer to clearance times in days (D), weeks (W), and months to years (Y).

D = maximal clearance half-times <1 day
W = maximal clearance half-times of a few days to a few months
Y = maximal clearance half-times of 6 months to several years

All actinides and transuranics (including americium) were placed in class Y. Lymphatic clearance applied to class Y, with two half-times governing the lymphatics. Ten percent of the material trapped in the lymph nodes had an effective half-time of 360 days, while the remaining 90% was presumed to be retained indefinitely and subject to radioactive decay only. As animal research studies produced clearance data, several more revisions of the model resulted. In 1972, all transplutonium oxides were assigned to class Y with pulmonary retention half-times of 500 days (ICRP 19). Deposition assumptions stated that 40% of class Y aerosols deposited in the pulmonary region were removed rapidly via the GI tract, 40% of deposited material was excreted via the GI tract, 15% was translocated to the lymph nodes, and the remaining 5% was cleared to the blood. ICRP Publication 19 also proposed for americium compounds that distribution should be 45% in the bone, 45% in the liver,and 10% in other tissues, or they should be excreted based on the very long clearance half-times for liver (40 yr) and whole body (100 yr).

In 1979, ICRP Publication 30 reclassified compounds of americium to class W to better agree with existing

animal data and follow-ups of accidental human inhalations (ICRP 30). For class W compounds, the model predicted that 20% to 30% of the inhaled particles would deposit in the pulmonary (P) compartment. Of this amount, 5% would translocate to the lymph (L), for a total of 1.25% of the inhaled particle deposition. A biological half-time of 50 days was assigned to the lymph, with all particles eventually clearing to the blood. This model, however, failed to predict the presence of long-term retained fractions observed in animal studies; the model also underpredicted fractions of lung deposits translocated to other organs including the tracheobronchial lymph nodes (TBLN) (Mewhinney 1982).

ICRP Publication 30 also established the Annual Limit of Intake (ALI) for inhaled americium as 5.4 nCi (200 Bq) (ICRP 30). ALI was defined as, "the activity of a radionuclide which taken alone would irradiate a person, represented by Reference Man, to the limit set by the ICRP for each year of occupational exposure" (ICRP 30).

Previous to this ICRP model, R. G. Thomas developed an interspecies model to compare clearance times between rodents and dogs (Thomas 1972). The model predicted an early loss from the upper respiratory tract of 1.5 days followed by intermediate clearance times such as 15 days

for rodents and a long term half-time of 400 days for dogs. Thus species differences existed and the amount of insoluble particles translocated to the lymph nodes also varied. This model innumerated the potential errors associated with using only animal studies to evaluate human lung clearances.

Animal Inhalation Studies

The decade of the 1960's witnessed a flurry of experimental activity concerning the fate of inspired plutonium, uranium, and americium. W. J. Bair et al. and Bair and Willard utilized dogs to observe the behavior of inhaled $^{239}PuO_2$ (Bair et al. 1962, Bair and Willard 1963). Both groups commented on the apparent continuous accumulation of plutonium in the TBLN. The highest activity occurred in the lungs followed by the TBLN with little activity in the skeleton or liver. Reported lung retention half-times were about 300 days and almost 1800 days for the whole body (Bair et al. 1962). Three probable clearance routes were suggested: fecal excretion, translocation to the TBLN, and translocation to other tissues with subsequent excretion in urine (Bair and Willard 1963).

W. J. Bair and R. W. Perkins investigated the feasibility of using ^{241}Am as a tracer for ^{241}Pu in the whole body monitoring of lung inhalations (Bair and Perkins 1968). After examining dog tissue, they noted a

slightly increased ^{241}Pu-^{241}Am ratio that suggested a relatively greater clearance of ^{241}Am but concluded no significant difference in Pu/Am clearance rates (Bair and Perkins 1968).

Several investigators using oxide compounds of plutonium and uranium reported on the translocation of the oxides to the TBLN. R. G. Thomas compiled available experimental data and plotted the ratio of pulmonary lymph node to lung concentration vs. time in days and found a distinct upward trend (Thomas 1968). Thomas interpreted this trend as representing a physiological or anatomical relation between lung clearance and the accumulation of insoluble particles in lymph nodes. L. J. Leach et al. in 1970 published a summary of a five year UO_2 inhalation study comparing retention and biological effects in monkey, dog, and rat (Leach et al. 1970). Two major sites of uranium were identified, the lung and the TBLN, that accounted for over 90% of the uranium found in the body. After one year, the uranium concentration continued to increase in the TBLN of the dog and monkey. At five years, the dog and monkey integrated alpha dose to the lung was estimated to be 500 and 900 rads, respectively, while the dose to the TBLN (both species) was estimated at 10,000 rads. W. J. Bair also noted the accumulation of PuO_2 in the TBLN having at least 40% of the initial deposition to the

alveoli (Bair 1970). The TBLN 5 to 6 years after exposure contained almost as much activity as the lung. Additionally, Bair observed translocation to other tissues, the liver and bone. He concluded that a slowly clearing deep compartment in the lung was feeding the TBLN.

C. L. Sanders and R. R. Adee postulated that inhaled, nonphagocytized particles may penetrate into the alveolar wall and accumulate. Therefore, these sequestered particles may partially explain the long residence time of plutonium in the lung (Sanders and Adee 1970).

R. G. Thomas et al. examined americium inhalation behavior in beagles using insoluble $^{241}AmO_2$ particles (Thomas et al. 1972). Translocation to the TBLN also occurred and the lymph nodes received the highest radiation dose; in one dog 1022 days after exposure, the dose was estimated to be 17,000 rads compared to 10,000 rads to the liver and 5300 rads to the lung. For one dog 127 days after exposure, 90% of the ^{241}Am oxide had cleared from the lung. J. A. Stanley et al. reported that lung retention appears to be species dependent and dogs retained a larger percentage of initially deposited ^{241}Am and ^{239}Pu than either the monkey or rat (Stanley et al. 1982). However, the researchers could not conclude statistically that differences in clearance

rates existed. They also observed that the TBLN was the only tissue other than the lung with significant amounts of plutonium and americium. This study raised the question of potential errors associated with using only dog data to predict insoluble particle behavior in humans. The data did, however, agree favorably with the ICRP Publication 30 lung model that predicted 20% to 30% of the inhaled activity deposited in the lung; the data by Stanley et al. showed 29% ±4%.

Human Inhalation Studies

Human subjects and inhalation victims present unique challenges for in vivo evaluation of insoluble actinide deposition and metabolism. In 1960, B. R. Fish postulated that with humans non-mobile uranium compounds would accumulate in the chest area, presumably in the pulmonary lymph nodes and other lymphatic tissue (Fish 1960). He further remarked that excretion data alone failed to sufficiently estimate the magnitude of the fixed deposition.

Accidental inhalations provide opportunites to monitor and observe lung clearance rates, biological half-times, and translocation to other tissues. Several human inhalations have occurred, but most studies provide inadequate data regarding TBLN concentration or translocation to the lymphatics. Early case histories concerning americium inhalation were reported by H. A.

May in 1968 (May 1968). The exposed man contained high count rates to suggest a body burden much greater than the maximum permissible level. Activity was distributed in the skeleton and bone as well as the lung.

Another accident involved inhalation of an americium-curium mixed oxide. S. M. Sanders described a rapid clearance phase by day 9 for americium (Sanders 1974). The researchers assumed 95% translocation from the lung via blood to bone with a 28-day biological half-time. TBLN activity was not determined. K. A. Edvardsson and L. Lindgren also found an initial, rapid clearance phase of americium in an accidental exposure (Edvardsson and Lindgren 1976). For the lung compartment, fast elimination occurred in the first days with an effective half-life of 2.5 days while the slower clearance occurred with a 17 day half-time. The authors also measured whole body activity and noted that the difference in lung and whole body half-times probably depended on relocation of activity in the body as well as calibration techniques. Moreover, the data suggested most of the migrating activity settled on bone tissue and in the liver.

R. E. Toohey and M. A. Esslig followed one accident case for 12 years and found 25% of the body burden in the chest area with most of this activity in the lungs; this distribution remained constant for the first 4

years with only a slight decrease (Toohey and Essling 1980). The authors noted that chelation therapy prevented them from drawing conclusions about americium metabolism, specifically TBLN accumulation. F. A. Fry measured two men for almost 4 years following an americium oxide inhalation (Fry 1976). The exposures were discovered several months after the event; therefore, rapid clearance rate patterns were unobserved. Whole body activity distribution changed with respect to time with the lung activity decreasing and the liver activity remaining constant, although the bone activity increased. Elimination from the chest area was slow with an estimated half-time of 900 days. No estimations were provided for TBLN accumulation.

D. Newton et al. in their study also found a long half-time of 900 days for residual activity located in the deep lung in a subject who inhaled a plutonium-americium mixed oxide aerosol (Newton et al. 1983). Additionally, 50% of the initial activity was removed in the first days via ciliary mechanisms. About 80% of the alveolar deposit cleared fairly rapidly, corresponding to a half-time of about 11 days. Although removal mechanisms via the blood and/or the lymphatics were effective, the role of the TBLN was not addressed.

Chapter 2. Materials and Methods

In the event of a human inhalation incident, insoluble particles probably deposit in the lung, and some particles may translocate to the TBLN. If any of these particles are radioactive, the activity located in the lung is usually measured. For this study, a human male subject with a known americium-241 lung activity of 2.4 nCi, was measured to determine if any of this activity had translocated from the lung to the TBLN.

Because the tracheobronchial lymph nodes are small (1 cm diameter or less) and occupy a narrow region around the trachea, this area needed to be isolated from the lungs. Lead sheeting was used to shield the detectors from scattered radiation and direct radiation from the lungs and, when the shield and detectors were centered over the TBLN, to detect effectively only radiation from the TBLN. This restricted counting area was designed to distinguish activity in the TBLN from activity in the lung.

Gamma Spectrometer Counting System

Counting was performed with two planar intrinsic germanium detectors (2000 mm^2 each) with intrinsic efficiencies of 74 to 76% each for americium-241. The active portion of each crystal had a diameter of 51 mm and was 13 mm thick. The end caps were stainless steel

tubing with beryllium windows (65-mm diameter, Ø.51-mm thick). Each detector was connected to a liquid nitrogen dewar, which was manually filled two times a week. The detectors were coupled to standard gamma spectrometer counting equipment; this system is part of the Whole Body Counting Unit at Battelle Pacific Northwest Laboratories (Palmer and Rieksts 1984, Palmer 1985).

The counting system was calibrated at the beginning of each workday or before counting measurements were made if the counts were done after normal work hours. A 95% enriched uranium-235 and americium-241 energy calibration source was used to calibrate the system at the energies of 185.5 keV (channel 371) and 59.6 keV (channel 119) for Ø.5 keV per channnel; counts were measured in 512 channels. The spectra consistently showed the highest number of counts in channel # 119 for the americium-241 sources.

The detectors were collimated with Ø.3-cm lead sheeting to restrict the counting area of the detector to a localized site. This thickness of lead was more than 15 times the mean free path of the 59.6 keV gamma:

> For a 59.6 keV gamma, the mass attenuation coefficient (μ/ρ) was determined by linear interpolation and was found to be 5.Ø6 cm^2/g (Storm and Israel 1967). Density of lead (ρ) is 11.34 g/cm^3. Thus the linear attenuation coefficient (μ) was 57.38 cm^{-1}. The mean free pathlength ($1/\mu$) of the 59.6 keV gamma was then Ø.Ø17 cm.

The collimator extended 10.1 cm below the bottom edge of the detectors (Figure 5); at the end of the collimator a 3.8-cm wide slot allowed the radiation to reach the detectors. The collimator extended 4.1 cm above the plane of the detector to shield the detectors laterally from scattered radiation.

Spectral Analysis

To find the gross photopeak counts, the number of counts in channels number 117 to 120 were summed (4 channels total). Background was determined by summing the counts in channels number 122 to 133 (total of 12 channels) and dividing by 3 (to average the counts over 4 channels, as in the gross photopeak number of channels). Net count rates (cpm) were found by:

$$\text{Net Count Rate} = \frac{\text{Gross Counts} - \text{Bkg. Counts}}{\text{Count Time (min).}}$$

The standard deviation of the net count rate was determined by:

$$1\sigma = \frac{(\text{Gross Counts} + \text{Background Counts})^{1/2}}{\text{Count Time (min).}}$$

Determination of Lower Limit of Detection

The lower limit of detection (LLD) expresses the effectiveness of a counting instrument in distinguishing between a measurement of true activity equal to zero and a measurement of true activity greater than zero, at a predetermined degree of confidence (Altshuler and

Figure 5. Lead collimator.

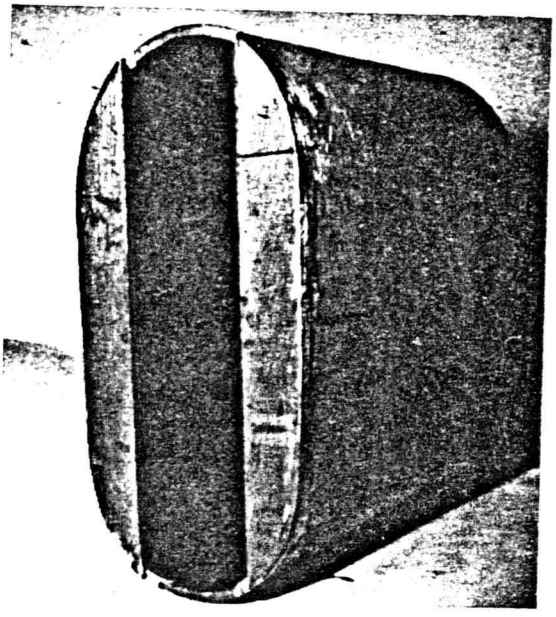

Pasternack 1963). The minimal activities are determined by evaluating the acceptability of making two types of statistical errors: Type I and Type II errors. A "Type I error states that true activity is greater than zero when, in fact, it is zero," and a "Type II error states that true activity is zero when, in fact, it is greater than zero" (Altshuler and Pasternack 1963). The probabilities, alpha and beta, of making these errors depend on the test procedure (for a Type I error) and the test procedure and amount of true activity (for a Type II error). Established values are given for acceptable alpha and beta probabilities. Constants associated with each probability, k-alpha and k-beta, are also given (Altshuler and Pasternack 1963):

alpha or beta	k-alpha or k-beta
0.005	2.576
0.010	2.326
0.025	1.960
0.050	1.645
0.100	1.282

By assuming alpha is equal to beta and also k-alpha is equal to k-beta, the following equation can be solved to determine the LLD (Currie 1968):

$$LLD = k^2 + 2k\ (2C_b)^{1/2}$$

where k (equal to k-alpha and k-beta) is a constant based on a predetermined probability; C_b is the number of background counts.

Low Background Counting Room

The low background counting room, or "the iron room", is built of slabs of steel (Roesch et al. 1960). Lead of 0.3-cm thickness lines the inner surface of the steel. The floor, walls, and ceiling are 25.4 cm thick, with the inner 17.8 cm being World War I battleship armor and the outer 7.6 cm being contemporary steel. The door of the room is the same thickness as the walls. The total floor space is about 3 by 3 meters; the ceiling is 2 meters high. A single concrete block wall partially surrounds the ground level building containing the iron room.

Tissue-Equivalent Phantom

A tissue-equivalent phantom (Figure 6), serial #C-108 (Palmer 1985), of a male torso containing americium-241 either in the lungs [620 nCi (22.9 kBq)] or in the TBLN [2200 nCi (81.4 kBq)] was counted on the ventral side with the collimated system (Griffith et al. 1979, Newton et al. 1985). "The phantom simulates a human male torso without head or arms and is terminated just above the pelvis. The stature is that of a man 1.77 m tall, weighing 76 kg. The phantom consists of a tissue-equivalent (TE) polyurethane torso shell with a human rib cage embedded therein" (Griffith et al. 1979). Lungs containing americium-241 (# 516) and an americium-241 point source for the TBLN (traceable to

Figure 6. A tissue-equivalent phantom with one chest-plate and internal organs.

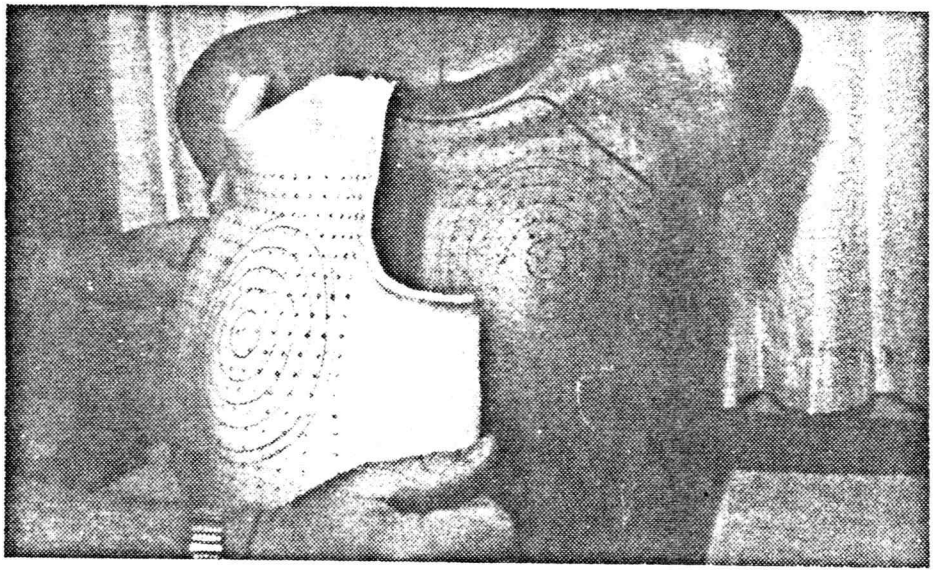

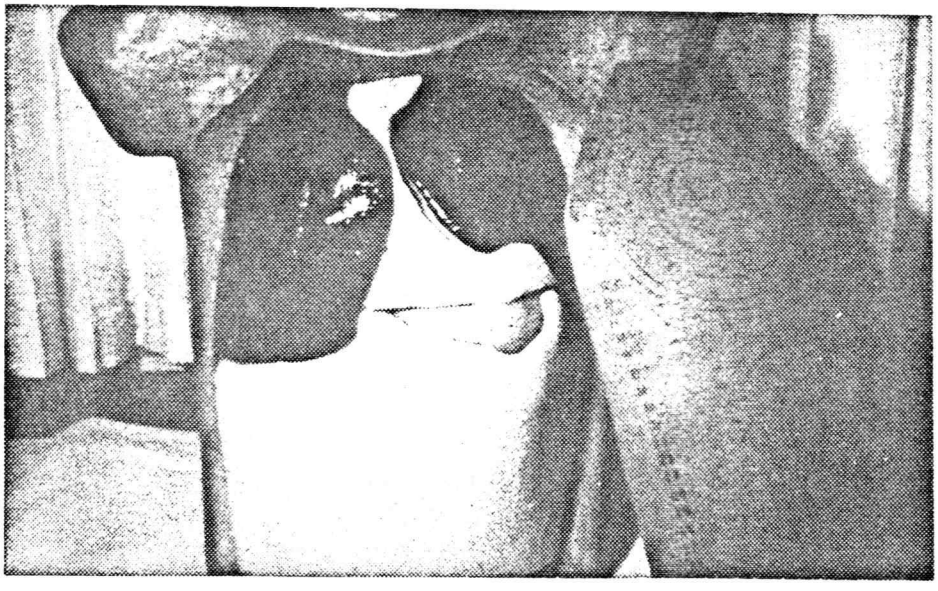

NBS) were used. Chest-wall thicknesses were varied by using chest-plates with different thicknesses and muscle-to-fat ratios (Table 1).

The phantom, generally placed in a horizontal position, was propped up about 4 cm with a laboratory block, placed between the scapula (shoulder blades). This position made the phantom more level and the surface more parallel with the collimator. The head of the male subject counted (see next section) was cushioned with a foam rubber pillow; this overall position of the subject closely matched the counting position of the phantom.

Human Male Subject

The human male subject was involved in an incident, inhaling insoluble plutonium-239 mixed with some plutonium-241. Americium-241, ingrown from plutonium-241, was also in the aerosol. Other details concerning the human male subject are deleted to maintain confidentiality.

Ultrasound Measurements

Chest-wall thickness of the male subject was measured by an ultrasound, real-time scanner. A Toshiba Sonolayergraph, SAL-1ØA, in the B mode was used. The probe (PL-5ØB) was the linear array type, operating at 5 MHz with a view width of 56 mm and a focal distance of

Table 1. Phantom chest-plate thicknesses and muscle-to-fat ratios.

Muscle/Fat Ratio	Plate Number	Average of Torso and Plate Thickness (cm)	Average Muscle %
13/87	A-119-CH1-119-1	2.26	76
	A-119-CH1-119-2	3.17	58
	A-119-CH1-119-3	3.58	53
	A-119-CH1-119-4	4.31	46
50/50	B-121-CH2-121-1	2.27	86
	B-121-CH2-121-2	2.87	78
	B-121-CH2-121-3	3.40	74
	B-121-CH2-121-4	4.14	70

Note: The phantom shell is 1.63 cm thick and 100% muscle.

24 mm. The ultrasound measurement was performed by Battelle personnel on June 29, 1984.

Ultrasound uses the principle of echolocation or the sending of ultrasounds into the environment and sensing the returning echos (Fleischer and Everette 1980). An ultrasound is a longitudinal pressure wave consisting of compressions and rarefactions in the material carrying the wave. The ultrasound is generated at a frequency greater than 18,000 Hz that is above the human range of hearing. Diagnostic ultrasound operates in the frequency ranges of 1 MHz to 25 MHz.

Piezoelectric crystals are used to generate and detect ultrasounds (Fleischer and Everette 1980). This crystal or transducer changes shape when an electric field is applied. Once the field is rapidly removed, the crystal returns to the resting state by oscillating and generating pressure waves into the medium. The frequency of the vibration depends on the crystal size; therefore, crystals are ground to vibrate at ultrasonic frequencies.

As the ultrasound propagates through a nonhomogenous medium, as in body tissue, the ultrasonic beam crosses interfaces that are the sites of change in acoustical impedance (Fleischer and Everette 1980). The acoustical impedence is related to the compressibility of the material, thus impeding the formation of compres-

sions and rarefactions. Density and elasticity of the tissue affect the degree of impedence. At the interface, a portion of the ultrasonic energy is reflected and returns as an echo to be detected by the transducer. In biological tissue, the waves travel at an average velocity of 1540 m/s and only require 6.5 milliseconds to move through 1 cm.

The ultrasound image is displayed on a cathode ray tube (CRT). The information collected by the transducer is amplified, with the resulting image composed of thousands of bright dots (Baum 1975). The returning echos are displayed as a graph. Distance along the Y-axis represents the time interval between each echo. Because the speed of the ultrasound through the tissues is known, time is converted to distance or thickness, as in the case of chest-wall measurements (Figure 7). The B mode of operation refers to intensity modulation or the brightness of the CRT dots representing the strength of the echo (Fleischer and Everette 1980).

Real-time imaging or scanning projects the ultrasound image as the interfaces change (Fleischer and Everette 1980). The linear array probe (transducer) contains an array or group of several crystals (McDicken 1976). Each crystal generates an ultrasonic pulse and receives the returning echos from the interfaces falling in its beam (Figure 8).

Figure 7. Ultrasound chest-wall thickness of a human male.

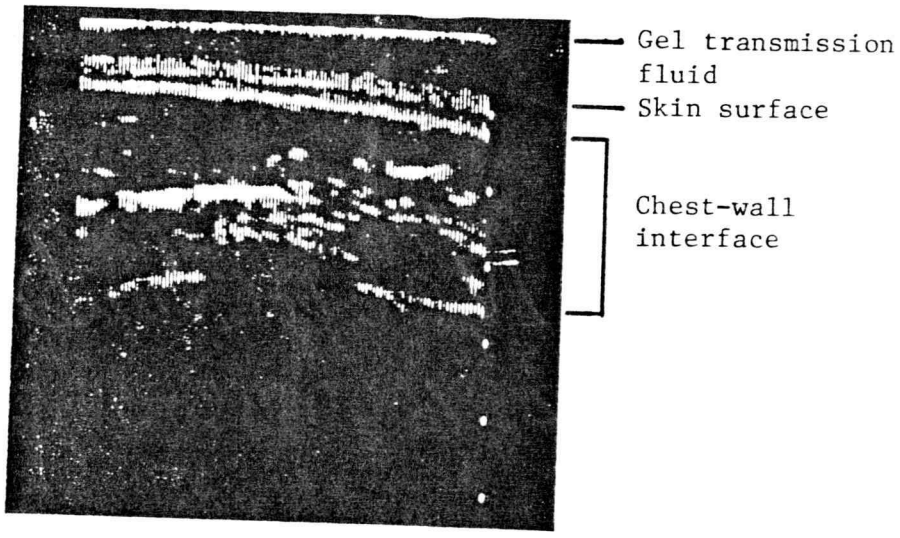

Figure 8. Array of crystals in a linear array probe (transducer) used in generating and receiving ultrasounds.

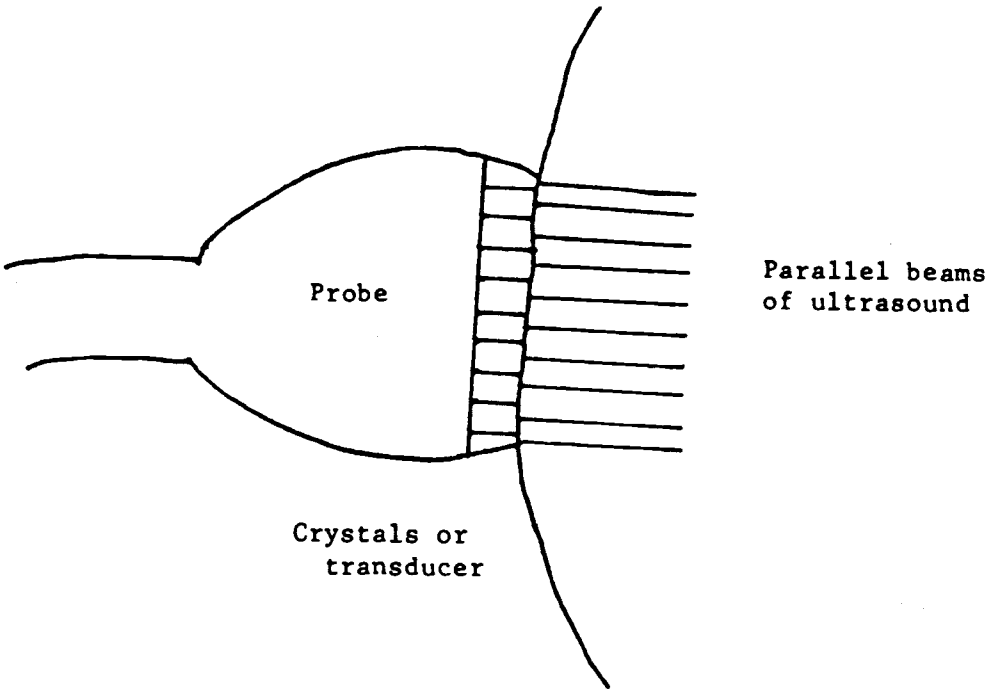

Counting Positions

To determine if the lead collimator would effectively restrict the radiation entering the detectors, seven counting positions were used on the ventral side of the phantom: CENTER over the sternum and TBLN; RIGHT 1, 2, and 3 over the three areas of the right lung; and LEFT 1, 2, and 3 over the three areas of the left lung (Figure 9). The 3.17 cm (13%-muscle 87%-fat) chest-plate was used for these measurements. The near edge of the collimator was placed just below the clavicle area. The collimator was lowered to rest lightly on the phantom chest. Counting times for each counting position varied from 10 to 15 minutes, depending on the source activity and the number of counts in the peak channel.

After initially counting the phantom, three counting positions were used on the ventral side of the phantom for the calibration curves: CENTER over the sternum and TBLN, RIGHT over the major area of the right lung, and LEFT over the left lung. Again, the near edge of the collimator was placed just below the bottom of the clavicle for each counting position (Figure 10). The collimator was lowered to rest lightly on the phantom chest. This placement was duplicated with the male subject. Counting times of thirty minutes were used with the phantom at each counting position, but 1-

Figure 9. The ventral side of the phantom with seven detector counting positions (with the 3.17 cm chest-plate: 13%-muscle 87%-fat).

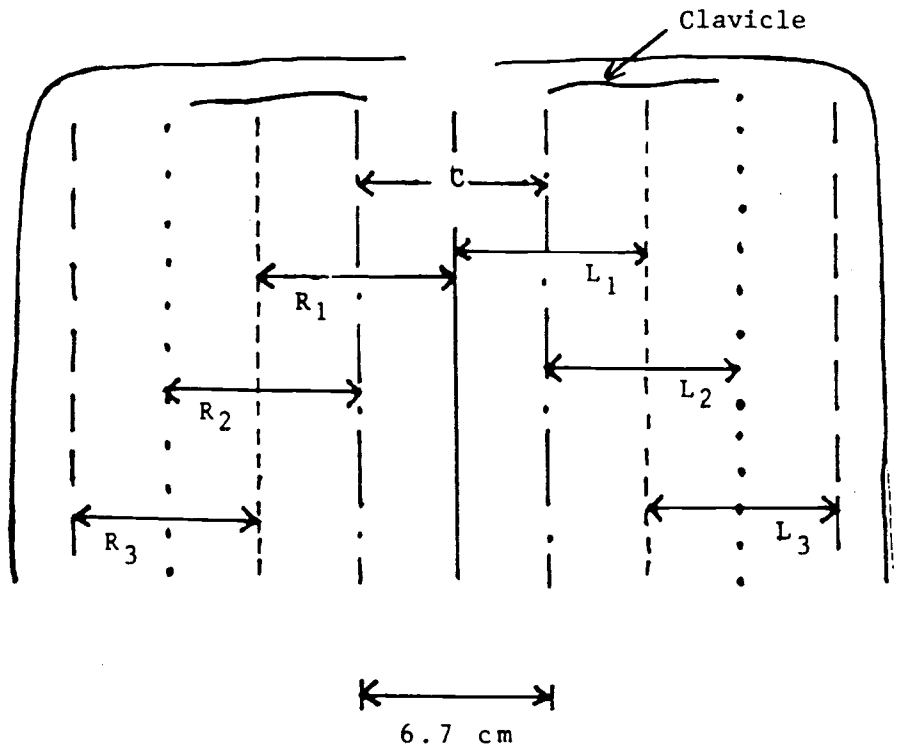

Figure 10. The ventral side of the phantom with three detector counting positions.

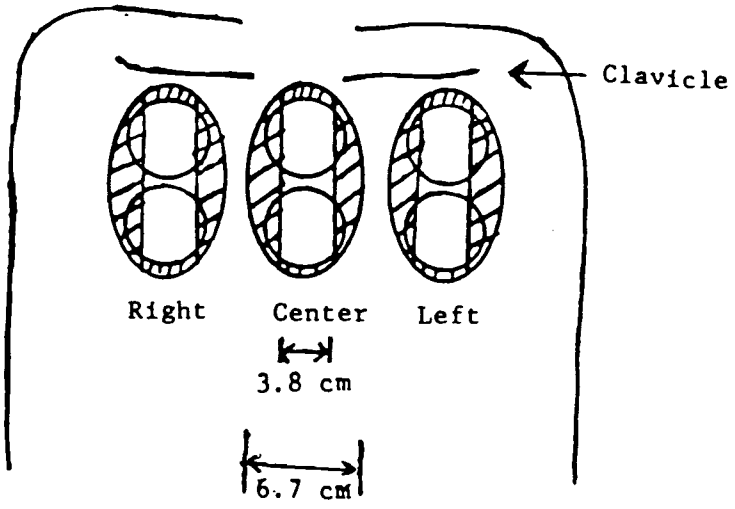

hour counting times were used with the male subject. Because the sources in the phantom were of high activity (lung: 620 nCi, TBLN: 2200 nCi), thirty minutes were sufficiently long enough to achieve good counting statistics. The low measured activity in the male subject (2.4 nCi) warranted a longer counting time to obtain reasonable counting statistics. One hour at each counting position was the longest counting time practicle for a human subject, considering the necessity for lying still during the counts, time away from the job, and reasonable counting statistics.

Chapter 3. Results

Initially, the phantom (with the 3.17 cm chest-plate) was counted for americium-241 activity in the seven counting positions, indicated in Figure 11 by the "100% lung" and the "100% TBLN" curves. These counting data showed that the collimated detection system distinguished activity in the lung from activity in the TBLN (Tables 2 and 3). The counting data for the male subject was also included in Figure 11. Two additional curves, (50% lung, 50% TBLN; 35% lung, 65% TBLN), shown in Figure 11, were generated by weighting the two measured sets of phantom counting data. These curves showed the effects of possible activity distributions between the lung and TBLN.

The phantom, for purposes of calibration, and the male subject were counted for americium-241 activity in the three counting positions: CENTER, RIGHT, and LEFT (Tables 4, 5, 6, 7, and 8). The LLD was determined for each counting set using probabilities of 0.025 for making Types I or II errors; all counts made were greater than the LLD. The phantom calibration curves show the relation between the net count rate per unit activity and chest-wall thickness (Figures 12, 13, 14, and 15). The muscle-to-fat ratios in the chest-plates minimally affect the slopes of the calibration curves; the deviation of the slopes for the two different

Figure 11. Phantom counting data curves for seven positions with the 3.17 cm chest-plate.

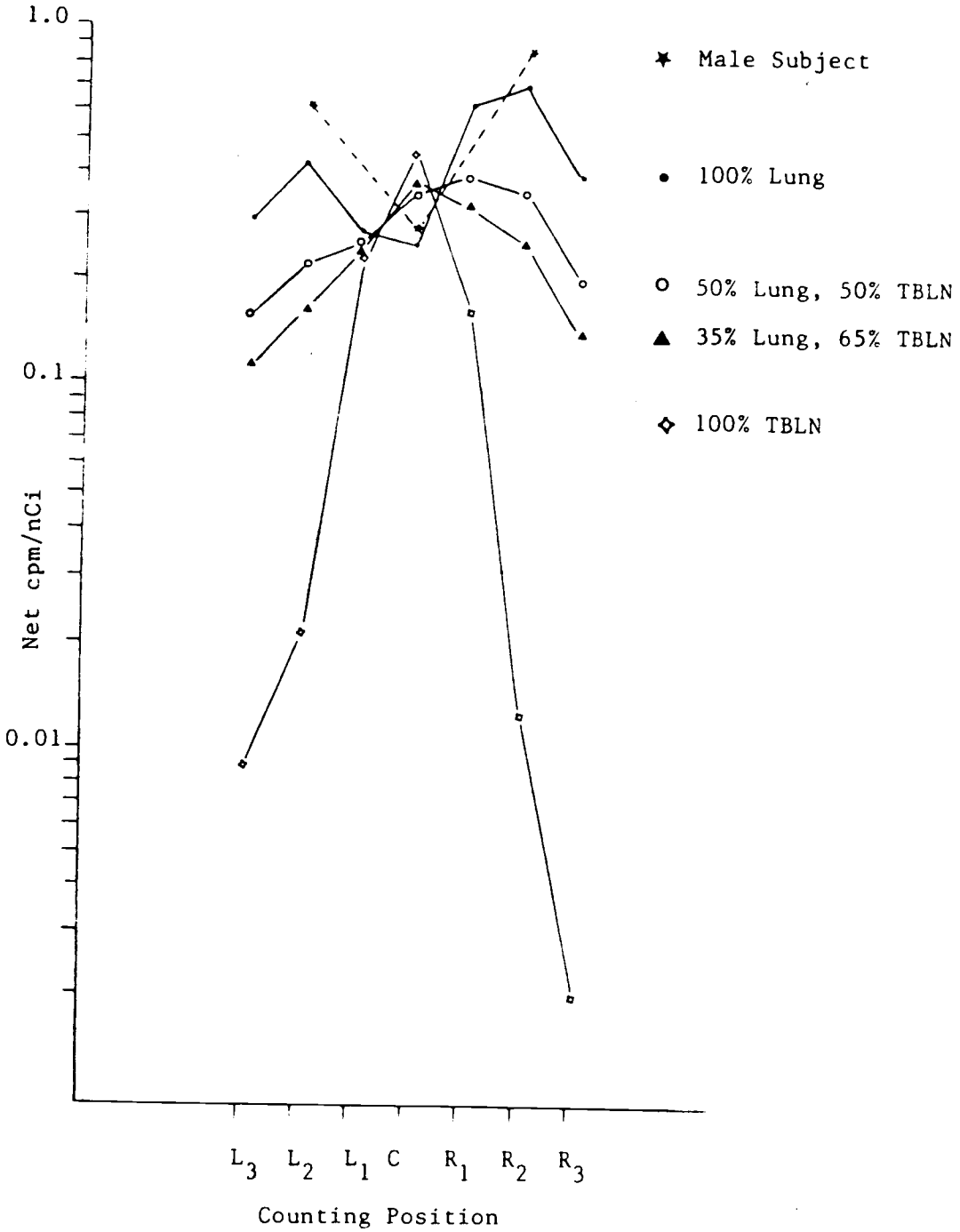

Table 2. Phantom counting data with the 3.17 cm chest-plate and the americium-241 (620 nCi) lung source.

Position	Count Time (min)	59.6 keV Cts.	Bkg. Cts.	Net cpm $\pm$ 1 σ	Net cpm per nCi
Center	15	2418	16	160.8 $\pm$ 3.3	0.259
L-1	12	2069	13	172.0 $\pm$ 3.8	0.277
L-2	12	3236	16	269.3 $\pm$ 4.7	0.434
L-3	12	2284	16	189.9 $\pm$ 4.0	0.306
R-1	12	4770	26	396.8 $\pm$ 5.8	0.640
R-2	12	5396	19	449.2 $\pm$ 6.1	0.725
R-3	12	3059	18	254.4 $\pm$ 4.6	0.410

Table 3. Phantom counting data with the 3.17 cm chest-plate and the americium-241 (2200 nCi) TBLN point source.

Position	Count Time (min)	59.6 keV Cts.	Bkg. Cts.	Net cpm $\pm$ 1 σ	Net cpm per nCi
Center	10	10294	20	1028.7 $\pm$ 10.1	0.468
L-1	12	6247	26	519.9 $\pm$ 6.6	0.236
L-2	12	553	12	45.8 $\pm$ 2.0	0.021
L-3	12	241	9	19.9 $\pm$ 1.3	0.009
R-1	12	4468	26	371.6 $\pm$ 5.6	0.169
R-2	12	361	23	29.5 $\pm$ 1.6	0.013
R-3	12	59	21	4.3 $\pm$ 0.7	0.002

Table 4. Phantom calibration counting data with the 13/87 chest-plates and the americium-241 (620 nCi) lung source.

Source and Counting Position	Plate Thickness (cm)	59.6 keV Cts. Ch. 117–120	Bkg. Cts. Ch. 122–133	Net cpm $\pm 1\sigma$
Lung: LEFT	1.63	11069	44	368.5 ± 3.5
	2.26	9356	53	311.3 ± 3.2
	3.17	7961	44	264.9 ± 2.4
	3.58	6920	50	230.1 ± 2.6
	4.31	5685	46	189.0 ± 2.5
Lung: CENTER	1.63	5319	45	176.8 ± 2.4
	1.63	4735	38	157.4 ± 2.3
	3.17	4231	48	140.6 ± 2.2
	3.58	3935	56	130.5 ± 2.1
	4.31	3405	43	113.0 ± 1.9
Lung: RIGHT	1.63	18905	38	629.7 ± 4.6
	2.26	15922	57	530.1 ± 4.2
	3.17	13319	53	443.4 ± 3.8
	3.58	12005	46	399.7 ± 3.7
	4.31	10160	38	338.8 ± 3.4

Note: All count times were for 30 min. The phantom torso shell is 1.63 cm thick and 100% muscle.

Table 5. Phantom calibration counting data with the 13/87 chest-plates and the americium-241 (2200 nCi) TBLN point source.

Source and Counting Position	Plate Thickness (cm)	59.6 keV Cts. Ch. 117-120	Bkg. Cts. Ch. 122-133	Net cpm $\pm 1\sigma$
TBLN: LEFT	1.63	495	41	16.0 $\pm$ 0.8
	2.26	543	47	17.6 $\pm$ 0.9
	3.17	565	43	18.4 $\pm$ 0.9
	3.58	591	41	19.2 $\pm$ 0.9
	4.31	614	53	19.9 $\pm$ 1.1
TBLN: CENTER	1.63	41335	56	1377.2 $\pm$ 6.8
	2.26	34453	56	1147.8 $\pm$ 6.2
	3.17	29619	49	986.8 $\pm$ 5.7
	3.58	26247	54	874.3 $\pm$ 5.4
	4.31	22046	41	734.4 $\pm$ 5.0
TBLN: RIGHT	1.63	8216	58	273.2 $\pm$ 3.0
	2.26	8148	43	271.1 $\pm$ 3.0
	3.17	7470	53	248.4 $\pm$ 2.9
	3.58	7169	41	238.5 $\pm$ 2.8
	4.31	6440	38	214.2 $\pm$ 2.7

Note: All count times were for 30 min. The phantom torso shell is 1.63 cm thick and 100% muscle.

Table 6. Phantom calibration counting data with the 50/50 chest-plates and the americium-241 (620 nCi) lung source.

Source and Counting Position	Plate Thickness (cm)	59.6 keV Cts. Ch. 117–120	Bkg. Cts. Ch. 122–133	Net cpm ± 1 σ
Lung: LEFT	1.63	11069	44	368.5 ± 3.5
	2.27	9329	42	310.5 ± 3.2
	2.87	7934	38	264.0 ± 3.0
	3.40	6678	48	222.1 ± 2.7
	4.14	5738	35	190.9 ± 2.5
Lung: CENTER	1.63	5527	64	183.5 ± 2.5
	2.27	4806	36	159.8 ± 2.3
	2.87	4407	40	146.5 ± 2.2
	3.40	4388	35	145.9 ± 2.2
	4.14	3521	49	116.8 ± 2.0
Lung: RIGHT	1.63	18905	38	629.7 ± 4.6
	2.27	15857	53	528.0 ± 4.2
	2.87	13803	39	459.7 ± 3.9
	3.40	11803	36	393.0 ± 3.6
	4.14	9750	50	324.4 ± 3.3

Note: All count times were for 30 min. The phantom torso shell is 1.63 cm thick and 100% muscle.

Table 7. Phantom calibration counting data with the 50/50 chest-plates and the americium-241 (2200 nCi) TBLN point source.

Source and Counting Position	Plate Thickness (cm)	59.6 keV Cts. Ch. 117–120	Bkg. Cts. Ch. 122–133	Net cpm $\pm$ 1 σ
TBLN: LEFT	1.63	495	41	16.0 $\pm$ 0.8
	2.27	522	35	17.0 $\pm$ 1.1
	2.87	560	47	18.1 $\pm$ 1.1
	3.40	719	45	23.5 $\pm$ 1.1
	4.14	591	41	19.2 $\pm$ 1.1
TBLN: CENTER	ENTER	41335	56	1377.2 $\pm$ 6.8
	2.27	34631	49	1153.8 $\pm$ 6.2
	2.87	29412	58	979.8 $\pm$ 5.7
	3.40	25903	50	862.9 $\pm$ 5.4
	4.14	21531	57	717.1 $\pm$ 4.9
TBLN: RIGHT	1.63	8216	56	273.2 $\pm$ 2.9
	2.27	7493	43	249.3 $\pm$ 2.9
	2.87	7394	51	245.9 $\pm$ 2.9
	3.40	6923	54	230.2 $\pm$ 2.8
	4.14	6246	44	207.7 $\pm$ 2.6

Note: All count times were for 30 min. The phantom torso shell is 1.63 cm thick and 100% muscle.

Table 8. Counting data of the male subject.

Counting Position	Chest Thickness (cm)	59.6 keV Cts. Ch. 117–120	Bkg. Cts. Ch. 122–133	Net cpm $\pm$ 1 σ
LEFT	2.95	125	105	1.5 $\pm$ 0.2
CENTER	2.95	75	100	0.69 $\pm$ 0.2
RIGHT	2.95	153	78	2.12 $\pm$ 0.2

Note: Counting times were for 60 min.

Figure 12. Phantom calibration data curves with the 13/87 chest-plates and the americium-241 (620 nCi) lung source.

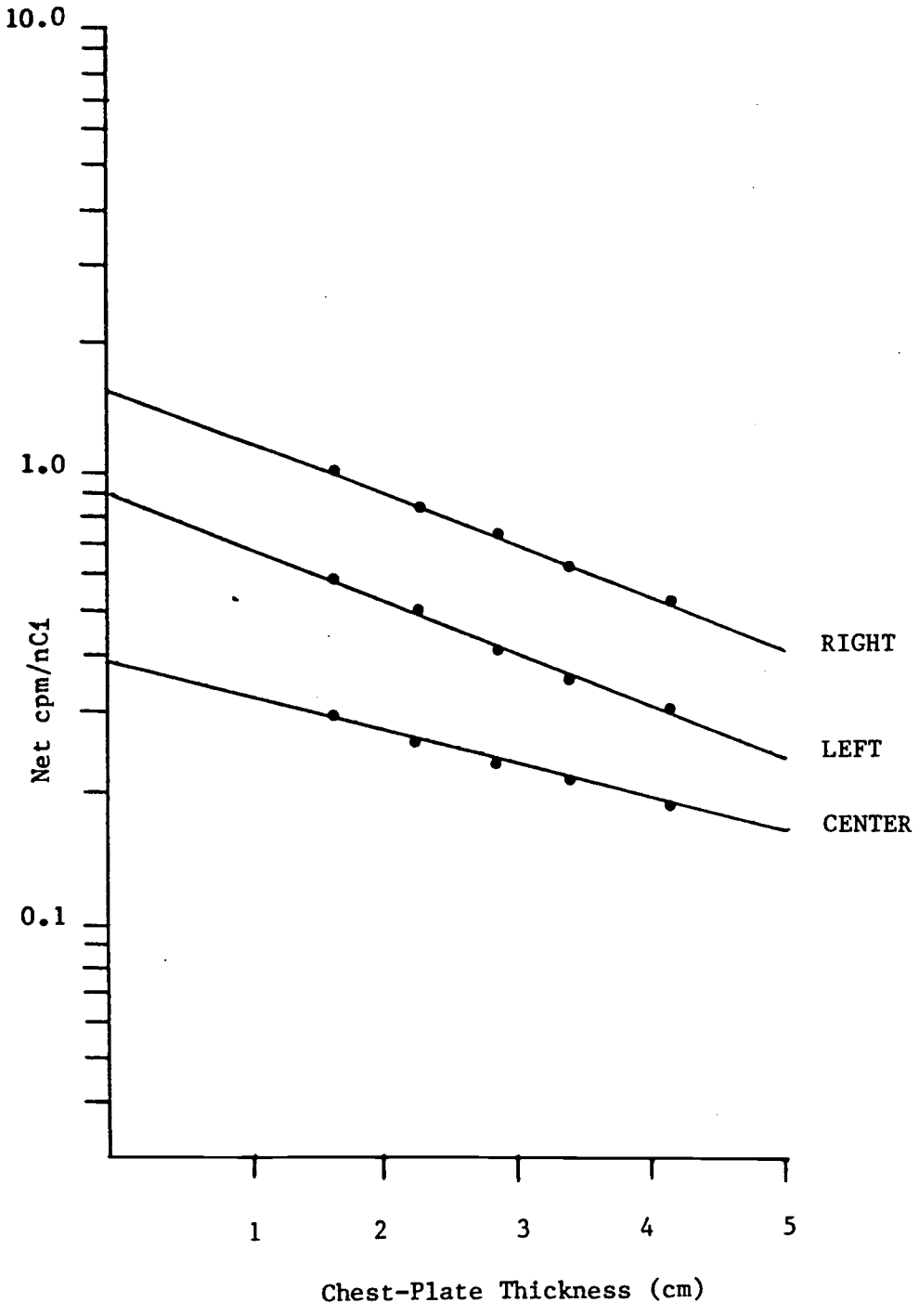

Figure 13. Phantom calibration data curves with the 50/50 chest-plates and the americium-241 (620 nCi) lung source.

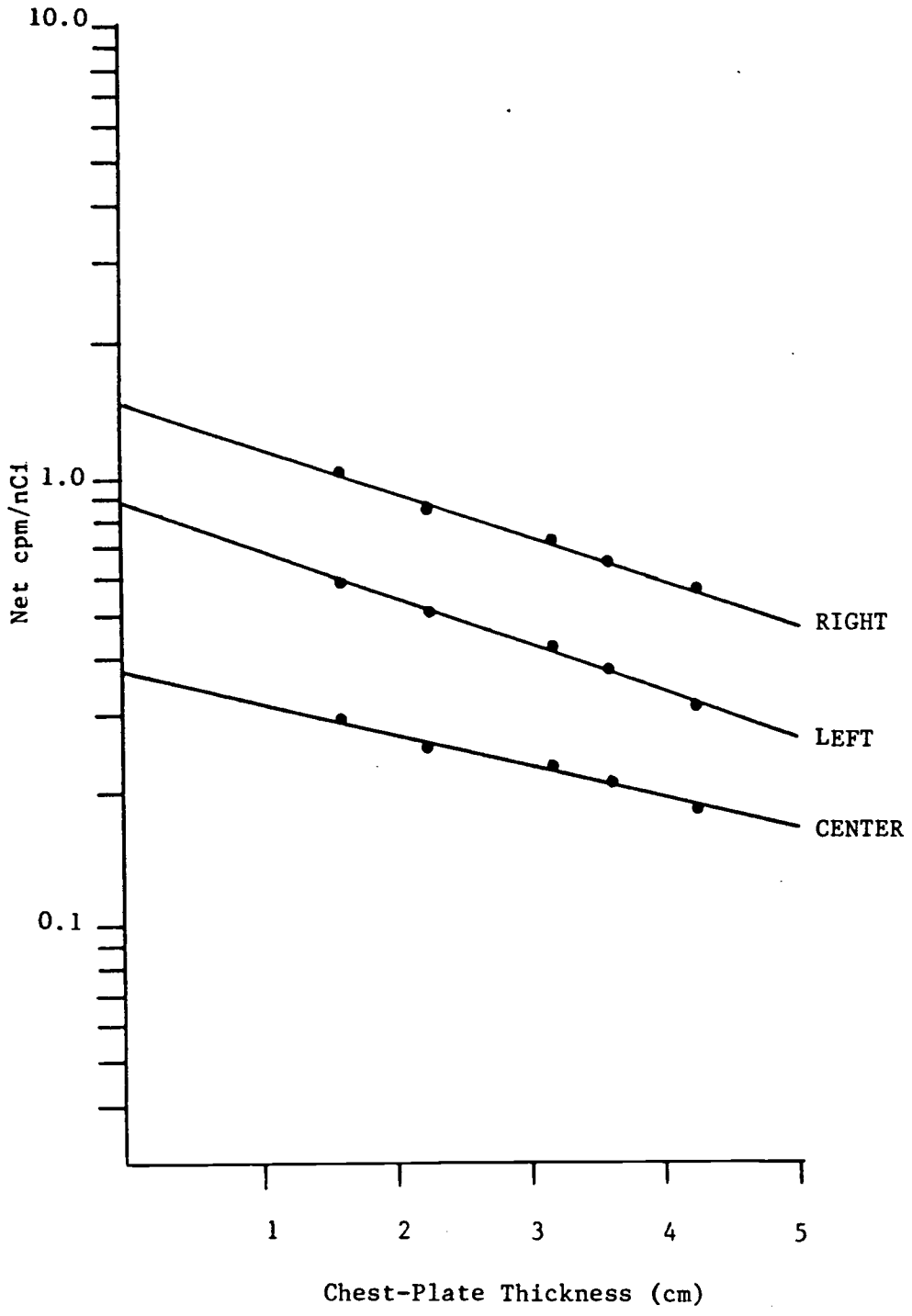

Figure 14. Phantom calibration data curves with the 13/87 chest-plates and the americium-241 (2200 nCi) TBLN point source.

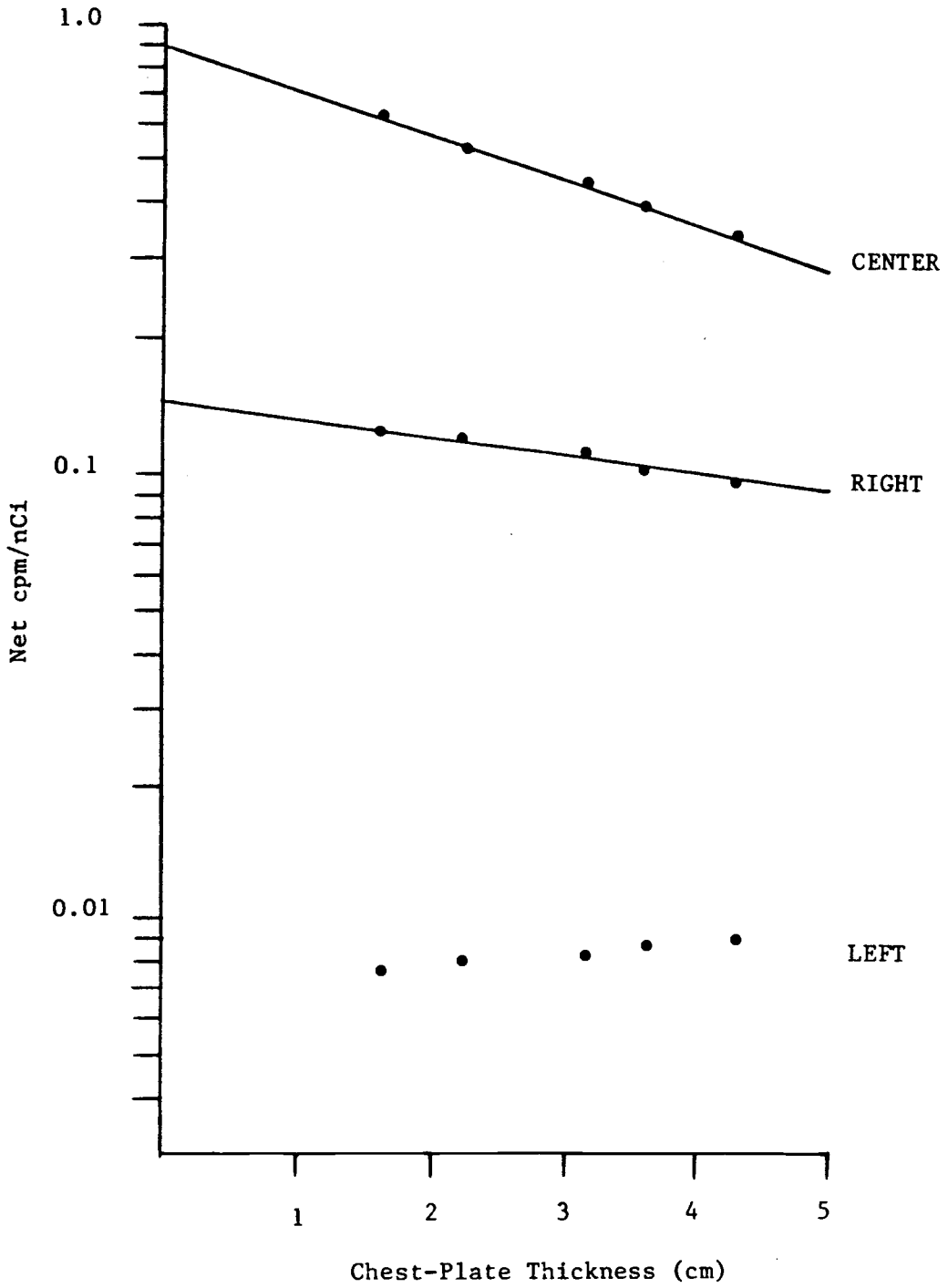

Figure 15. Phantom calibration data curves with the 50/50 chest-plates and the americium-241 (2200 nCi) TBLN point source.

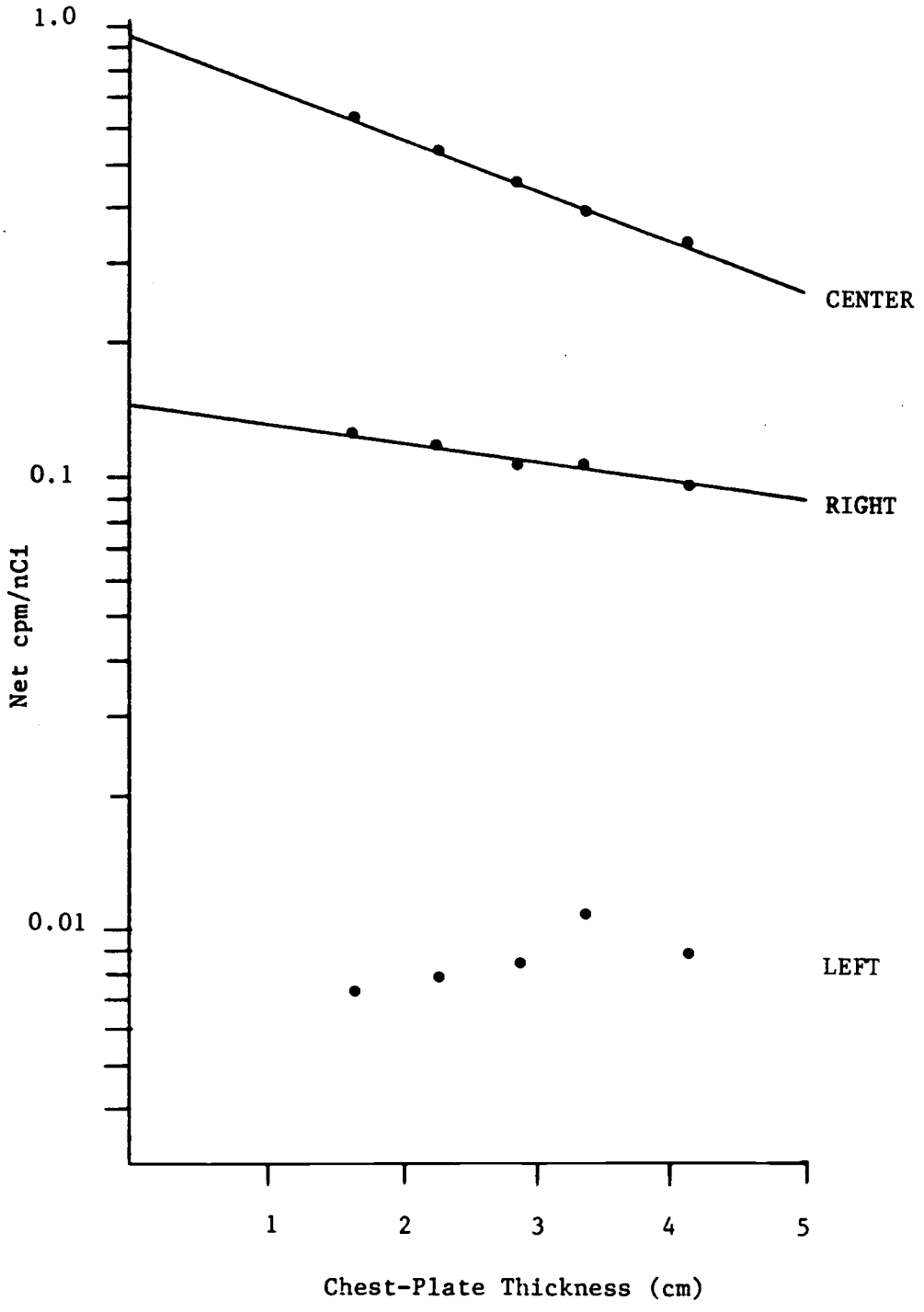

muscle-to-fat ratios (Tables 9 and 10) varies from 13.8% (RIGHT,Lung) to 1.6% (CENTER,Lung).

For the CENTER and RIGHT positions, increased chest-wall thickness decreased the net count rate per unit activity to give a negative slope; as expected, this result was found for both the lungs and the TBLN sources. The lung source in the LEFT counting position showed a negative slope. For the TBLN point source, however, the LEFT counting position showed an increased net count rate per unit activity as chest-wall thickness increased (positive slope). Thus the LEFT position measurements were inconsistent between the lung and TBLN sources and were not used to determine the activity distribution.

Activity in the lungs (L) and TBLN (T) comprise the total activity in the chest. For a given chest-wall thickness of interest, curves in Figures 12 through 15 give values in net cpm/nCi for the lung (λ) and TBLN (τ) for each counting position. The net counts per minute (C), λ , and τ for the CENTER and RIGHT counting positions were used to determine the activity in the lungs and the TBLN by the following equations:

$$C_C = \lambda_C L + \tau_C T \qquad (1)$$

$$C_R = \lambda_R L + \tau_R T \qquad (2)$$

where the subscripts C and R are for the CENTER and RIGHT counting positions.

Table 9. Intercepts and slopes for the phantom calibration data with the 13/87 chest-plates.

Organ	Position	Intercept (A) (net cpm/nCi)	Slope (B) (cm−1)	Correlation Coefficient (R**2)
Lung	LEFT	0.8863	−0.2431	0.991016
	CENTER	0.3708	−0.1616	0.992049
	RIGHT	1.4574	−0.2278	0.997779
TBLN	LEFT	0.0065	0.0779	0.954551
	CENTER	0.8977	−0.2275	0.992586
	RIGHT	0.1483	−0.0916	0.938716

Note: y = A exp (B * X) where X is a given chest-wall thickness.

Table 10. Intercepts and slopes for the phantom calibration data with the 50/50 chest-plates.

Organ	Position	Intercept (A) (net cpm/nCi)	Slope (B) (cm−1)	Correlation Coefficient (R**2)
Lung	LEFT	0.9155	−0.2675	0.995638
	CENTER	0.3837	−0.1637	0.938363
	RIGHT	1.5605	−0.2637	0.999126
TBLN	LEFT	0.0062	0.1068	0.496011
	CENTER	0.9477	−0.2594	0.998924
	RIGHT	0.1465	−0.1026	0.963193

Note: y = A (exp B * X) where X is a given chest-wall thickness.

Solving for lung activity (L) and TBLN activity (T) yields:

$$L = \frac{C_R \tau_C - C_C \tau_R}{\lambda_R \tau_C - \lambda_C \tau_R} \quad (3)$$

$$T = \frac{C_C - \lambda_C L}{\tau_C} \quad (4)$$

Net count rates for the male subject were Ø.69 cpm (CENTER) and 2.12 cpm (RIGHT).

To determine the errors associated with the calibration curves, the uncertainties (δ) were calculated for the intercept (δ A) and the slope (δ B). The uncertainty for the chest-plate thicknesses and the ultrasound chest-wall measurement (δ x) were assumed to be $\pm$ Ø.Ø5 cm. The following equation determined the error for each calibration coefficient, $\delta\lambda$ and $\delta\tau$, as indicated by δy:

$$\delta y = e^{bx} \left(\delta a^2 + a^2 x^2 \delta b^2 + a^2 b^2 \delta x^2 \right)^{1/2}$$

The variable, x, was the chest-wall measurement (2.95 cm) for the male subject.

Once the uncertainties for the calibration coefficients were determined, the propagation of error was found for a function of several variables. These variables, counting statistics (1σ), $\delta\lambda$, $\delta\tau$, and δ x were assumed to be independent. Thus, if F is a function of random variables x, y, z ..., then F(x,y,z...) is a random variable with a standard

deviation (1) given by (Falk 1976, Jaffey 1960):

$$\sigma_F = \left[\left(\frac{\delta F}{\delta X}\right)^2 \delta X^2 + \left(\frac{\delta F}{\delta Y}\right)^2 \delta Y^2 + \left(\frac{\delta F}{\delta Z}\right)^2 \delta Z^2 + \cdots\right] \qquad 6)$$

By solving Equation (6), the uncertainty was determined for each measured activity:

50/50 Plates			13/87 Plates		
Lung	2.96 ± 0.36	nCi	Lung	2.84 ± 0.34	nCi
TBLN	-0.025 ± 0.47	nCi	TBLN	0.079 ± 0.45	nCi

Both the 50/50 and the 13/87 muscle-to-fat calibration curves were used to determine λ_C, λ_R, τ_C, τ_R, (Figures 12, 13, 14, and 15) and to solve for T and L by Equations (3) and (4) for the male subject. This method showed a slight difference in lung activity between the two calibration curves. The 50/50 curves indicate a lung activity of 2.96 nCi (110 Bq) and a TBLN activity of -0.025 nCi (0 Bq). The 13/87 curves give an activity of 2.84 nCi (105 Bq) for the lung and an activity of 0.079 nCi (2.9 Bq) for the TBLN.

The general physique of the male subject more closely matched the 50/50 chest-plates than the 13/87 plates. Fat percentage in the chest area of the subject (chest thickness of 2.95 cm) was estimated to be a maximum of 15%, using the ultrasound pictures of the chest. The 50/50 plate at 2.87 cm has an overall muscle average of 78% (or 22% fat). The 13/87 plate at 3.17 cm has a muscle average of 58% muscle (or 42% fat). Thus the activities of 2.96 nCi (110 Bq) for the lungs and

-0.025 nCi (0 Bq) for the TBLN are considered more representative of the male subject.

Americium-241 activity in the lung in the male subject measures 2.4 nCi, according to a measurement performed by Battelle personnel on October 25, 1985. Six intrinsic germanium detectors were used for the counting measurement. Three detectors were placed over each lung; the counts were summed and averaged to determine the chest activity.

The americium-241 produced in a plutonium-241 aerosol is trapped in the physical matrix of the plutonium particles (Palmer 1985). Americium, therefore, does not translocate independently of the plutonium. For this study, americium was considered to behave like plutonium, a class Y compound.

The ICRP Publication 30 model predicts fractions of material deposited in each region of the respiratory system, clearance half-times, and clearance routes. For class Y compounds in the pulmonary (lung) region, four distinct compartments house the deposited particles, each section with a clearance half-time (T in days), compartmental fraction (F), and clearance route:

Compartment	Route	T	F
e	body fluids	500	0.05
f	T-B region & GI tract	1.0	0.4
g	T-B region & GI tract	500	0.4
h	Lymph area	500	0.15

The lymph area clears into the lymph nodes; two compartments comprise the lymph nodes:

Compartment	Route	T	F
i	body fluids	1000	0.9
j	remain in nodes	∞	0.1

For class Y compounds, particle loss from the lung region is due to a short clearance phase (f) and long clearance phases (e), (g), and (h). These longer phases can be considered as a single clearance mechanism with a fraction of 0.6, because they all have the same clearance half-time, as shown in Equation (7):

$$\frac{dN_L}{dt} = -0.6\,\lambda_L N_L - 0.4\,\lambda_f N_L \qquad (7)$$

where N_L is the number of americium-241 atoms in the lung, λ_L and λ_f are the clearance constants associated with the 500 day and 1.0 day clearance half-times from the lung, and t is the time since the initial uptake in days. The initial condition $N_L(0) = N_L^\circ$ was assumed. The shorter clearance phase (f) is negligible; the solution to Equation (7) becomes:

$$N_L(t) = N_L^\circ e^{-0.6\,\lambda_L t} \qquad (8)$$

Particle clearance from the lung to the lymph area results in a buildup of particles in the lymph nodes. Particles in the lymph nodes leave by a relatively long clearance phase (i) or are retained indefinitely (j). Equation (9) accounts for particles cleared from the lung into the lymph nodes and clearance out of the nodes:

$$\frac{dN_{LN}}{dt} = 0.15\,\lambda_L N_L(t) - 0.9\,\lambda_{LN} N_{LN} \qquad (9)$$

where N_{LN} is the number of americium-241 atoms in the TBLN, λ_{LN} is the clearance constant for the 1000 day clearance half-time from the TBLN. The initial condition $N_{LN}(0) = 0$ was assumed.

Substitution of Equation (8) into Equation (9) yields:

$$\frac{dN_{LN}}{dt} = 0.15\,\lambda_L \left(N_L^{\circ} e^{-0.6\lambda_L t}\right) - 0.9\,\lambda_{LN} N_{LN} \qquad (10)$$

Solving Equation (10) yields:

$$A_{LN} = \frac{0.15 A_L^{\circ}\,\lambda_L}{0.9\,\lambda_{LN} - 0.6\,\lambda_L}\left(e^{-0.6\lambda_L t} - e^{-0.9\lambda_{LN} t}\right) \qquad (11)$$

where $A_L^{\circ} = \lambda_p N_L^{\circ}$, $A_{LN} = \lambda_p N_{LN}$, and λ_p is the radiological decay constant for americium-241.

Values of λ_L and λ_{LN} are given by:

$$\lambda_L = \ln 2/500 \text{ d} = 13.86 \times 10^{-4} \text{ d}^{-1}$$

$$\lambda_{LN} = \ln 2/1000 \text{ d} = 6.93 \times 10^{-4} \text{ d}^{-1}$$

This study was conducted about 8 years (2920 days) after the initial uptake. Substitution of these values into Equation (11) yields a ratio of:

$$\frac{A_{LN}}{A_L} = 0.073$$

According to the ICRP 30 model for class Y compounds, therefore, about 7% of the particles deposited in the lung is expected to translocate out of the lung into the lymph nodes within a time period of 8 years.

Chapter 4. Discussion

The collimated counting system effectively restricted the radiation entering the detectors; only a localized area of either the lungs or TBLN was counted. Generally, widely scattered radiation was removed from the counting field, and americium-241 activity in the lungs was distinguished from activity in the TBLN.

Low energy photons are absorbed readily in tissue; for example, the half-value layer for the plutonium-239 17 keV uranium L x-ray is 6 mm (Campbell and Anderson 1979). Moreover, human chest-wall thickness varies fron 1 to 4.5 cm, and percentage of fat in chest-walls varies from 10% to 30% with a mean of 22% (Campbell and Anderson 1979). Campbell and Anderson measured fat percentages in humans and plotted calibration curves showing the relation between detection efficiency and fat content. The curves give percent of change in detection efficiency for any chest-wall thickness vs. the percentage of fat content in the chest-wall. The authors concluded this method allows them to predict changes in detection efficiency. Therefore, it seems that varying fat content in the chest-wall results in different detection efficiencies and would affect count rates.

In this study, phantom calibration curves of net count rate per unit activity vs. chest-wall thickness

for different muscle-to-fat ratios showed minor variation (14% maximum) between the 50%-muscle 50%-fat chest-plates and the 13%-muscle 87%-fat plates. The muscle-to-fat ratio appeared nearly insignificant in this method of calibration (results varied about 4% for the two sets of plates).

The calibration curves, however, showed the importance of detector position on the phantom and male subject. Newton et al. (1985) report on using the phantom as a calibration standard for measuring plutonium activity in human lungs. The study compares results between U. S. Department of Energy laboratories (Lawrence Livermore National Laboratory, Battelle Pacific Northwest Laboratories, and Argonne National Laboratory) and government labs in England (Harwell and Atomic Energy Research Establishment). The authors note that the left lung to right lung mass ratio is 0.77:1, with a relative radioactivity distribution ratio of about 0.8. But the observed relative counts from the phantom (for two phoswich detectors) are lower with a mean left-to-right ratio of 0.3. The ratio for the human subjects counted, having a ^{92m}Nb lung activity, is about 0.6. The smaller size of the left lung and the screening by the heart cause this asymmetrical response. Newton et al. concluded the phantom exaggerates this response.

Counting data from the TBLN calibration curves also showed an asymmetrical response. The heart, a large muscle mass, is located on the left side; radiation from the TBLN point source apparently was attenuated and scattered by the heart. Scattered radiation seemed to affect the LEFT TBLN calibration curve more than attenuated radiation, causing a slightly positive slope.

Craig et al. (1979) and Thomas et al. (1972) used beagles to study the metabolism of inhaled, insoluble americium-241 aerosols and measured particle translocation to the thoracic lymph nodes. Craig et al. find retention values in the lymph nodes of <1%, and Thomas et al. measure 0.14% retention in dogs sacrificed about the same number of days after exposure. Craig et al. noted that americium-241 is translocated in lower amounts than reported amounts of plutonium oxide translocated (often 40 to 50%) in dogs.

The counting data for the male subject, related to the phantom calibration curves, showed minimal to insignificant americium-241 activity in the TBLN. The errors for the lung and TBLN activities indicated that the TBLN percentage of total chest activity ranged from highs of 18% (50/50 plates) and 21% (13/87 plates) to a low of 0% (both sets). This collimated-detector counting method appeared useful for a qualitative assessment in determining if translocation had occurred.

The qualitative evaluation was enhanced by using quantitative techniques to derive the activities and errors.

These data generally agreed with the beagle studies; americium-241 was not translocated to the human TBLN in nearly (if at all) the amounts observed with plutonium oxides in dogs (Craig et al. 1979).

Monthly routine chest measurements of the male subject during 1985 indicate an americium-241 chest activity range from 2.0 nCi to 2.6 nCi (Palmer 1985). Typically, the error was $\pm$ 0.10 nCi (1 σ) for each of these measurements. The error associated with this low activity mainly depends on counting statistics (Falk 1976). Battelle personnel also assume a 10% detector positioning error, but this assumption was not considered in the reported error.

The ICRP 30 lung dynamics model predicts that 7% of the particles initially deposited in the pulmonary (lung) region translocates to the lymph nodes in an 8 year time period. The measured lung activity for the 13/87 chest-plates (2.84 nCi) and the TBLN activity (0.079 nCi) indicated about 3% translocation from the lung to the TBLN, although the 1 σ range of error associated with these values varies from 0 to 17%. This range of error agreed reasonable well with the ICRP 30 model prediction.

The concept of the critical organ concerns the part of the body that is most susceptible to radiation damage under specific conditions. For inhaled plutonium and other actinides, the critical organ is the lung. ICRP Publication 30 asserts that the irradiation of the lung is more likely to be the limiting factor for inhaled, insoluble radioactive particles (ICRP 30). Because in animal studies neoplasia (tissue destruction) has been observed rarely in lymphatic tissue, even though the plutonium concentration was greater than the lung concentration, the Main Commission of the ICRP recommends "that lymphatic tissue should not be considered the critical organ in inhalation exposure to plutonium" (ICRP 19). The commission, however, recognizes that no long-term exposure experiments have been conducted wiht amounts of plutonium or americium that may favor the development of lymphoid tumors. Until animal experiments indicate severe lymphoid tissue damage at low plutonium concentrations, the lung will remain the critical organ.

Because the activity in the TBLN was negligible for both sets of chest-plates, the lung measurement was considered to represent the total chest activity. The method used in this study to measure the lung activity, therefore, indicated a total chest activity of 2.96 nCi (50/50 plates) or 2.84 nCi (13/87 plates). These values

were within the range reported by Battelle. The difference in total chest activity between the two measurements (this study and Battelle's) appeared to be insignificant.

The conclusions of this study were as follows:

1) For the phantom calibration counting data, the collimated detection system has been found to be useful in distinguishing activity in the lung from activity in the TBLN.

2) For human subjects with low (nCi range) measured chest activity, this technique provides a reasonable qualitative evaluation of possible translocation, supported by quantitative assessment.

3) The measured activity from the male subject generally supported the ICRP 30 model translocation prediction for class Y compounds.

Bibliography

Altshuler B. and Pasternack B., 1963, " Statistical measures of the lower limti of detection of a radioactivity counter," Health Phys. **9**, 293-298.

Bair W. J., Willard D. H., Herring J. P. and George L. A., 1962, "Retention, translocation and excretion of inhaled $Pu^{239}O_2$," Health Phys. **8**, 639-649.

Bair W. J. and Willard D. H., 1963, "Plutonium inhalation studies-III. Effect of particle size and total dose on deposition, retention and translocation," Health Phys. **9**, 253-266.

Bair W. J. and Perkins R. W., 1968,"Plutonium-americium ratios in dogs after inhalation of $^{239}PuO_2$," in: Pacific Northwest Laboratory Annual Report, BNWL-714 (Richland, WA: Pacific Northwest Laboratory).

Bair W. J., 1970, "Long-term $^{239}PuO_2$ studies," in: Plutonium Inhalation Studies, BNWL-1221 (Richland, WA: Pacific Northwest Laboratories).

Baum G., 1975, Fundamentals of Medical Ultrasonography (G. P. Putnam's Sons: New York), 474 p.

Campbell G. W. and Anderson A. L., 1979, "New developments in ultrasonic imaging of the chest and other body organs," in: Advances in Radiation Protection Monitoring, IAEA-SM-229/53 (IAEA: Vienna).

Craig D. K., Park J. K., Powers G. J. and Dennis L. C., 1979, "The deposition of americium-241 oxide following inhalation by beagles," J. Radiat. Res. **78**, 455-473.

Currie L. A., 1968, "Limits for qualitative detection and quantitative determination," Anal. Chem. **46**, 586-593.

Eckert R. and Randall D., 1983, Animal Physiology. Mechanisms and Adaptions, second edition (W. H. Freeman and Company : New York), 830 p.

Edvardsson K. A. and Lindgren L., 1976, "Elimination of americium-241 after a case of accidental inhalation," in: Diagnosis and Treatment of Incorporated Radionuclides, STI/PUB/411 (Vienna: IAEA).

Falk R. B., 1976, "Error analysis and propagation of uncertainities for the measurement of inhaled transuranium elements," in: Proceedings of the Workshop on Measurement of Heavy Elements In Vivo, K. L. Swinth, ed. (Battelle Pacific Nortwest Laboratories: Richland, WA), 277 p.

Fish B. R., 1960, "Inhalation of uranium aerosols by mouse, rat, dog and man," in: Inhaled Particles and Vapors, (New York: Pergamon Press, Inc.).

Fleischer A. C. and Everette J. Jr., 1980, Introduction to Diagnostic Sonography (John Wiley & Sons: New York), 339 p.

Fraser R. G. and Pare J. A. P., 1971, Organ Physiology. Structure and Function of the Lung (W. B. Saunders Company: Philadelphia), 115 p.

Fry F. A., 1976, "Long-term retention of americium-241 following accidental inhalation," Health Phys. **37**, 13-20.

Griffith R. V., Dean P. N., Anderson A. L. and Fisher J. C., 1978, "Tissue-equivalent torso phantom for inter-calibration of in vivo transuranic-nuclide counting facilities," in: Advances in Radiation Monitoring, IAEA-SM-229/56 (Vienna: IAEA).

ICRP Publication 19, 1972, The Metabolism of Compounds of Plutonium and Other Actinides (Pergamon Press: Oxford), 59 p.

ICRP Publication 30, 1979, Limits for Intakes of Radionuclides by Workers, Part 1 (Pergamon Press: Oxford), 116 p. and Supplement to Part 1 (Pergamon Press: Oxford), 555 p.

Jacquez J. A., 1979, Respiratory Physiology, (Hemisphere Publishing Corporation: Washington), 442 p.

Jaffey A. H., 1960, "Statistical tests for counting," Nucleonics **18**, 180-184.

Leach L. J., Maynard, E. A., Hodge H. C., Scott, J. K., Yuile C. L., Sylvester G. E. and Wilson H. B., 1970, "A five-year inhalation study with natural uranium dioxide (UO_2) dust-I. Retention and biolgical effect in the monkey, dog and rat," Health Phys. **18**, 599-612.

May H. A., 1968, "Preliminary report on the distribution of americium-241 following accidental inhalation," ANL-7489 (Argonne, IL: Argonne National Laboratory).

McDicken W. N., 1976, Diagnostic Ultrasonics: Principles and Use of Instruments (Crosby Lockwood Staples: London), 320 p.

Mewhinney J. A., Griffith W. C. and Muggenburg B. A., "The influence of aerosol size on retention and translocation of ^{241}Am following inhalation of $^{241}AmO_2$ by beagles," Health Phys. **42**, 611-627.

Morrow P. E.,1980, "Lymphatic drainage of the lungs," in: Pulmonary Diseases and Disorders, Vol. I by A. L. Fishman (McGraw-Hill Book Company: New York), pp. 272-274.

Murray J. A., 1976, The Basis for Diagnosis and Treatment of Pulmonary Disease (W. B. Saunders Company: Philadelphia), 334 p.

Nagaishi C., 1972, Functional Anatomy and Histology of the Lung (Igaku Shoin Ltd.: Toyko), 295 p.

Newton D., Taylor, B. T. and Eakins, J. D., 1983, "Differential clearance of plutonium and americium oxides from the human lung," Health Phys. **44**, 431-439.

Newton D., Wells, A. C. and Toohey, R. F.,1985, "Livermore phantom as a calibration standard and assessment of plutonium in lungs," in: Assessment of Radioactive Contamination in Man, IAEA-SM-276/01 (Vienna: IAEA).

Oppenheimer J. R., 1947, "The Atomic Age," in: The Scientists Speak, edited by W. Weaver (Boni and Gaer: New York), 369 p.

Palmer H. E., 1985, Personal Communication, Battelle Pacific Northwest Laboratories, Richland, Washington.

Palmer H. E. and Rieksts G., 1984, "The use of planar high purity Ge detectors for in vivo measurement of low-energy photon emitters," Health Phys. **47**, 569-578.

Park J. F., Bair W. J. and Busch R. H., 1972, "Progress in beagle dog studies with transuranium elements at Battelle-Northwest," Health Phys. **22**, 803-810.

Roesch W. C., McCall R. C. and Palmer H. E., 1960, Hanford Whole Body Counter 1959 Activities, HW-67045 (General Electric: Richland, WA).

Sanders C. L. and Adee R. R., 1970, "Ultrastructural localization of inhaled $^{239}PuO_2$ particles in alveolar epithelium and macrophages," Health Phys. **18**, 293-295.

Sanders S. M., 1974, "Excretion of ^{241}Am and ^{244}Cm following two cases of accidental inhalation," Health Phys. **27**, 359-365.

Schulz W. W., 1976, Chemistry of Americium, DOE-TID-2-6971, 300 p.

Shepo D., Belamarich F. and Levy C., 1974, Human Anatomy and Physiology. A Cellular Approach (Holt, Rinehart and Winston, Inc.: New York), 622 p.

Stanley J. A., Edison A. F. and Mewhinney J. A., "Distribution, retention and dosimetry of plutonium and americium in the rat, dog and monkey after inhalation of an industrial-mixed uranium and plutonium oxide aerosol," Health Phys. **43**, 521-530.

Storm E. and Israel H. I., 1967, Photon Cross Sections from 0.001 to 100 MeV for Elements 1 through 100, USAEC Report LA-3753 (Los Alamos, NM: Los Alamos Scientific Laboratory).

Stuart B. O., 1984, "Deposition and clearance of inhaled particles," Env. Hlth. Persp. **55**, 369-390.

Task Group on Lung Dynamics, 1966, "Deposition and retention models for internal dosimetry of the human respiratory tract," Health Phys. **12**, 173-209.

Thomas R. G., 1968, "Transport of relatively insoluble materials from lung to lymph nodes," Health Phys. **14**, 111-117.

Thomas, R.G., 1972, "An interspecies model for retention of inhaled particles," in: Fundamentals, Applications, and Implications to Inhalation Toxicity, edited by T. T. Mercer, P. E. Morrow, and W. Stober (Springfield, IL: Charles C Thomas), pp. 405-420.

Thomas R. G., McClellan R. O., Thomas R. L., Chiffelle T. L., Hobbs C. H., Jones R. C., Mauderly J. L. and Pickrell J. A., 1972, "Metabolism, dosimetry, and biological effects of inhaled ^{241}Am in beagle dogs," Health Phys. **22**, 863-871.

Toohey R. E. and Essling M. A., 1980, "Measurments of ^{241}Am in vivo at long times after inhalation," Health Phys. **38**, 139-145.

Weibel, E. R., 1980, "Design and structure of the human lung," in: Pulmonary Diseases and Disorder, Vol. I by A. P. Fishman (McGraw-Hill Book Company: New York), pp. 224-271